Investigating the Role of VGF and its Associated Neuropeptides in Post-stroke Recovery and Repair

Hannah Gillis

Thesis submitted to the University of Ottawa
In partial fulfillment of the requirements for the degree of
Master of Science

Department of Biochemistry, Microbiology and Immunology

Faculty of Medicine
University of Ottawa

Abstract

The high incidence of stroke worldwide as well as the poor efficacy of neuroprotective drugs has shifted the focus of research towards therapies targeting stroke recovery and rehabilitation. VGF (non-acronym), a secreted protein that is processed into several neuropeptides, has been identified as a post-stroke repair molecule playing a role in neurogenesis and the modulation of neuroinflammation. In the present study, we assess the requirement for VGF and its specific peptides during post-stroke neurogenesis and behavioural recovery. Using a photothrombotic stroke model we induced stroke in the left frontal cortex of wild type and VGF cKO mice. Following stroke, behavioral tests were performed to measure sensorimotor deficits over a four-week period. Finally, mice were sacrificed and used to assess the levels of neurogenesis and neuroinflammation at timepoints ranging from 1-28 days post-stroke. We have used gain- and loss-of-function experiments to demonstrate that VGF and its derived peptides can improve recovery following photothrombotic stroke in the sensorimotor cortex. Preliminary results indicate that VGF peptides increase mobilization of NSCs from the ventricular zone. Further investigation is required to define the precise mechanism underlying the functional recovery and to fully determine the effectiveness of VGF as a relevant therapeutic for post-stroke recovery in the future.

Acknowledgements

I would firstly like to thank my supervisor Dr. David Picketts for his continued guidance, support and expertise. If he didn't know the answer, he was always able to direct me towards someone that could. I would also like to thank the current and former members of the Picketts lab for their expertise in areas I was unfamiliar, as well as their assistance in trouble shooting, sample preparation and most importantly their moral support. I'd also like to thank my friends and family for their time and patience throughout the completion of this degree. The many holidays, weekends, events and priorities that have taken a back seat throughout the past few years, I am so grateful for their continued support.

Table of Contents

List of Abbreviations

AD = Alzheimer's disease
ALS = Amyotrophic lateral sclerosis
ANOVA = analysis of variance
ATP = adenosine triphosphate
BDNF = brain derived neurotrophic factor
cDNA = complementary deoxyribonucleic acid
cKO = conditional knockout
CNS = central nervous system
CSF = cerebral spinal fluid
DCX = doublecortin
DNA = deoxyribonucleic acid
ER = endoplasmic reticulum
FOV = field of view
GnRH = gonadotropic releasing hormone
GPCR = G-protein coupled receptor
GTG = gold thioglucose
HPLC = high performance liquid chromatography
MCI = mild cognitive impairment
MDD = major depressive disorder
MRI = magnetic resonance imagine
NGF = nerve growth factor
P = postnatal
PCR = polymerase chain reaction
PGK = phosphoglycerate kinase
PVDF = polyvinylidene difluoride
qPCR = quantitative polymerase chain reaction
RNA = ribonucleic acid
SDS-PAGE = sodium-dodecylsulfide polyacrylamide gel electrophoresis
SVZ = subventricular zone
tPA = tissue plasminogen activator
VZ = ventricular zone
WT = wildtype

List of Figures

List of Tables

1. Introduction

1.1 Neuropeptides

Neuropeptides are small, hormone-like proteins that are produced or secreted by neuronal cells after cleavage of full-length proteins, that participate in regulated pathways in the central nervous system (CNS) of most mammalian species[1]. In *homo sapiens*, there are over 100 neuropeptides synthesized in the soma, processed and packaged into dense core vesicles to be transported down the axon and dendrites. The signalling molecules are released in a calcium-dependent fashion and bind to G-protein coupled receptors (GPCR) to induce further cell signalling[2,3]. This class of peptides are among one of the most diverse groups of signalling molecules and play a major role in a variety of physiological processes throughout the body[1].

1.2 VGF

1.2.1 Discovery and expression patterns

VGF, also known as 'Plate 5 Nerve Growth Factor Inducible gene' was discovered in 1985 by Levi *et al.* in a study of rat pheochromocytoma PC12 cells examined for transcriptional responses after treatment with nerve growth factor (NGF)[4]. The gene sequence previously classified as *vgf8a* was upregulated 50-fold in cultured PC12 cells after prolonged exposure to NGF. The VGF gene was later shown to be present on chromosome 7, containing 3 exons and encoding a 615 amino acid protein (*homo sapiens*) that was part of the secretogranin/chromogranin family[5,6] (**Figure 1**). Upon further investigation, VGF was shown to be secreted by neuroendocrine cells throughout the central nervous system with highest expression in brain tissue[7]. Later studies showed that other growth factors including

neurotrophin-3 (NT-3) and brain-derived neurotrophic factor (BDNF) could also influence VGF expression[7,8]. The growth factor BDNF has been shown to support the production and survival of newborn neurons within the hippocampus during periods of exercise[9]. BDNF also participates in a positive-feedback loop with VGF, intrinsically regulating their expression in an activity dependent manner[10]. VGF expression has also been shown to be expressed in an activity dependent manner in mouse models of cerebellar ataxia and depression[11,12].

1.2.2 Peptides

Upon its secretion, VGF is enzymatically cleaved by prohormone convertases 1/3 and 2 into multiple smaller, biologically active peptides[13] (**Figure 2**). These peptides have been shown to play major roles in a variety of biological processes, the most notable being reproduction, brain repair, metabolism and energy maintenance. Arguably the most well characterized peptides, TLQP-62 and TLQP-21 have previously been shown to be involved in neurological processes such as neurogenesis and cell survival respectively[14,15]. Other well characterized peptides NERP-1 and 2 (Neuroendrocrine regulatory peptide) have been shown to influence body fluid homeostasis in rats through the regulation of vasopressin release[16].

1.2.3 VGF receptors

Fundamentally, neuropeptides such as VGF signal through GPCRs to activate cell signalling pathways and downstream targets. Two GPCRs identified for VGF peptides are complement receptors C3aR and gC1qR[17,18]. The C-terminal VGF peptide TLQP-21 was shown to bind to adipocyte membranes through a single class of binding sites and a cell-

Figure 1. Schematic of VGF gene. The 615 amino acid protein (617 in mice) encoded by the VGF gene before cleavage into smaller peptides. Untranslated sequence of VGF is interrupted by two introns, with exon three encoding the VGF protein.

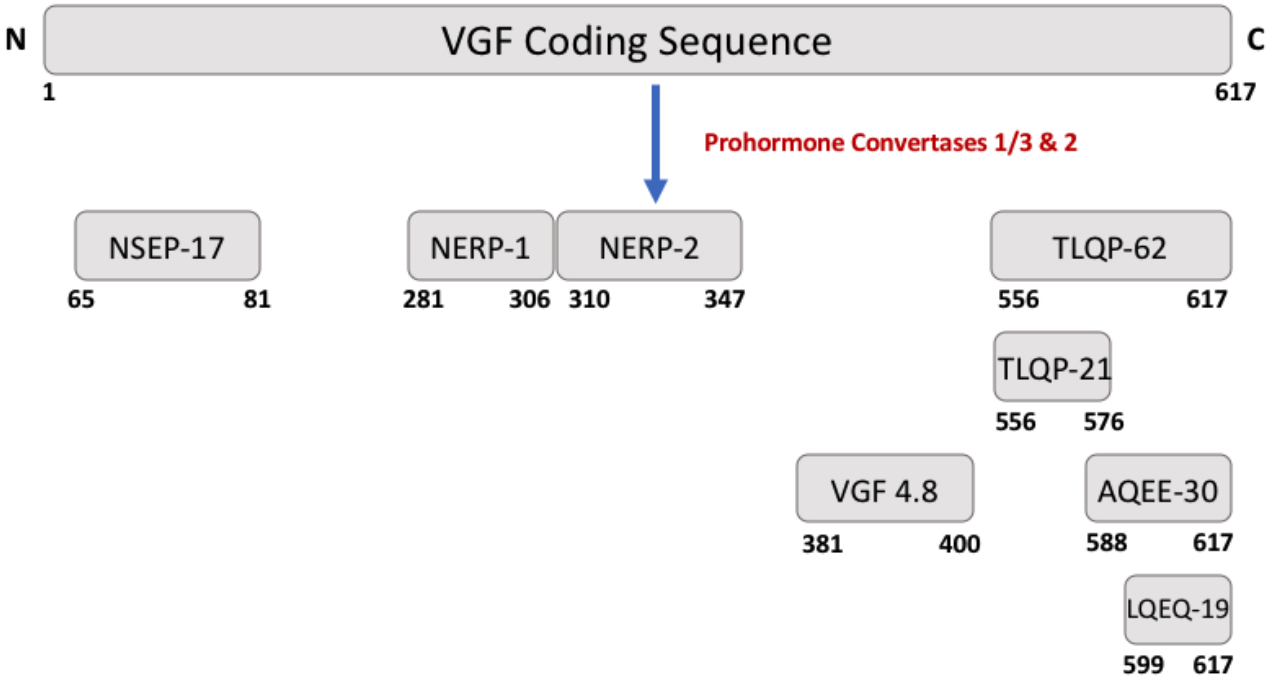

Figure 2. Diagrammatic view of VGF-derived peptides. Prohormone convertases 1/3 and 2 convert full-length VGF peptide into smaller, biologically active peptides. C-terminal peptides are known to be more biologically active. Total number of derived peptides is unknown.

surface receptor[19,20]. Further investigation showed that TLQP-21 is structurally similar to complement protein C3a, allowing it to bind through its' cell-surface receptor C3aR[17]. It is proposed that TLQP-21 also signals through the globular head of the C1q receptor, although no proposed mechanism or structural similarity has been shown[18,71].

1.3 VGF mouse models

1.3.1 Knockout models

To delineate the role of VGF in multiple biological processes investigators have utilized a number of different knockout mouse models which have displayed very distinct phenotypes. One of the earliest homozygous knockout mouse models of VGF used a phosphoglycerate kinase-(PGK-) driven neomycin resistance cassette to replace the entire VGF coding sequence. These mice displayed a hypermetabolic phenotype and were resistant to lesion-, diet- and genetically induced obesity[21]. Similarly, later studies also using a homozygous transgenic model resulted in infertile, hypermetabolic and excessively lean mice with very little fat storage capacity[22]. Additional findings showed that heterozygous VGF knockout mice presented with decreased adiposity, increased energy expenditure and resistance to obesity[22]. These findings supported the notion that VGF is imperative for the proper functioning of metabolism and energy maintenance.

Upon closer examination of the neurological effects of VGF ablation, knockout mouse models have demonstrated that VGF also plays a significant role in hippocampal development and function. Both heterozygous and homozygous knockout mice generated from the same PGK-transgene as previously mentioned displayed impaired spatial learning, memory and contextual fear conditioning tasks[23]. These findings suggested that VGF could modulate synaptic transmission via a BDNF-dependant mechanism[23].

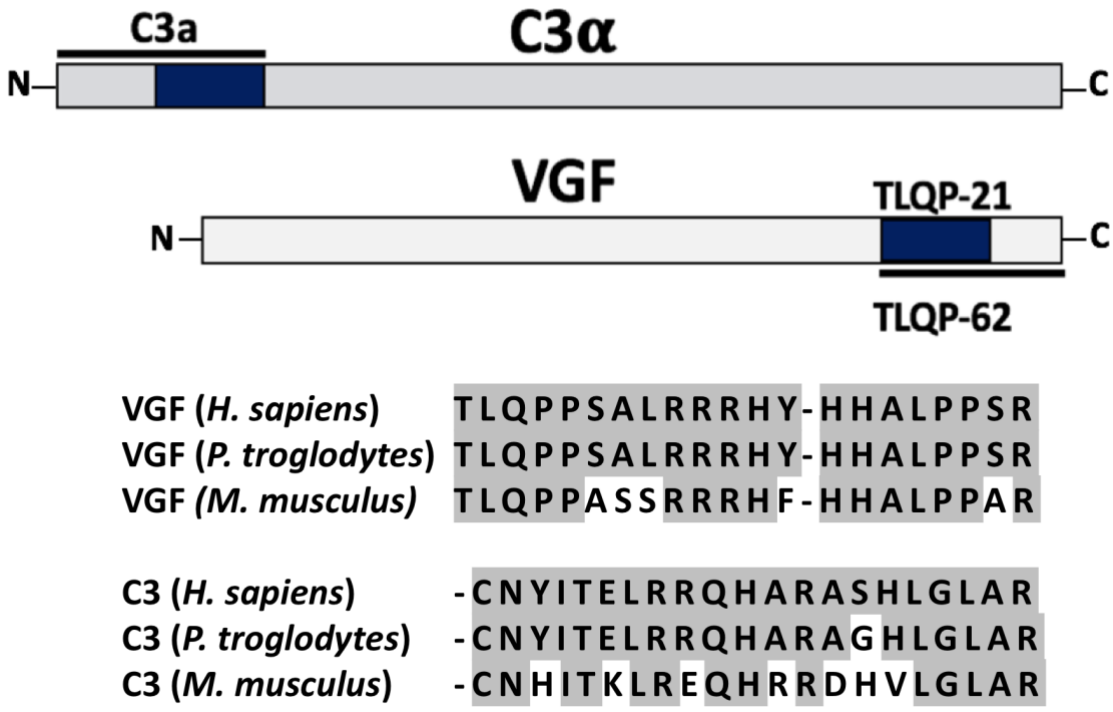

Figure 3. TLQP-21 is structurally similar to C3a. The C-terminal VGF peptide has similar structural properties to complement proteins C3 and are conserved among species.

1.3.2 Overexpression models

Overexpression models of VGF have provided support for a role for VGF in several biological processes. A model of exogenous overexpression of VGF administered C-terminal peptide TLQP-21 to Siberian hamsters through intracerebroventricular infusion[24]. These mice demonstrated a slight increase in energy expenditures and body temperature, along with a significant decrease in body weight comparable to knockout models previously mentioned[7,25]. A more traditional model of overexpression using a VGF transgene under the control of a ubiquitous promoter resulted in no significant changes in body weight, contrary to the exogenous model of overexpression[26]. This difference observed between these two models might suggest that there is a difference in the effects of systemic and resident overexpression patterns. These mice did, however, have a slight difference in their brain weight attributed to enlarged lateral ventricles and a reduction in striatal volume, not attributed to cell death[26]. Further characterization of these mice showed that they demonstrated depressive tendencies, impaired memory as well as hyperactivity.

1.4 Functional Roles of VGF

VGF and its secreted peptides have consistently been shown to be important mediators of a variety of biological mechanisms and processes, playing a functional role in their execution and regulation. VGF-derived peptides have been shown to be involved in the regulation of energy homeostasis, metabolism and fat storage in mouse models along with the pathology of multiple neurological disorders and processes such as neuroprotection, neuroinflammation and nociception. Determining the scope of VGF-derived peptides and their involvement in the

mediation of these processes has given greater insight into the pathology of several neurological disorders.

1.4.1 Metabolism and energy maintenance

One of the earliest discoveries of VGF and its biological effects was that of metabolism and energy maintenance. Early studies looking at mice in the fed state, showed normal colocalization of VGF mRNA in the ARC nuclei with α-MSH, whereas fasting mice showed increased VGF expression and colocalization[21,27]. More recent evidence demonstrates that VGF expression is altered in the ARC nuclei of Siberian hamsters after altering their circadian pacemaker, affecting metabolism and body weight[28,29]. Early VGF knockout models, although appearing normal at birth, showed a significantly reduced growth curve and weighed 40-60% less than wildtype littermates at weaning[21]. In fact, these mice were also shown to be hypermetabolic, consuming 50% more O_2, while daily intake of food was equivalent to wildtype littermates[30,31].

More recent mouse models assessed VGF and its effect on diet-induced obesity[27]. Ablation of the VGF gene prevented the metabolic effects typically induced by a high-fat diet on the body weight and circulating leptin levels in mice[31]. Alternatively, using a gold thioglucose (GTG) model of obesity in VGF knockout and wildtype mice, the targeted deletion of VGF prevented the increase in obesity seen in the wildtype mice[32,33]. These findings led to the conclusion that VGF is a key mediator of nutrition, metabolism and energy homeostasis.

1.4.2 Reproduction

The hypermetabolic effects seen in mice with altered VGF expression have also been closely associated with delayed sexual maturation and infertility. It has also been suggested that altered VGF expression resulting in reduced fat storage and altered metabolism may have the ability to

cause a deficiency in the production and secretion of gonadotropic releasing hormone (GnRH), a key mediator of the reproductive process[34,35]. GnRH is one of the most crucial hormones secreted as part of the hypothalamic-pituitary-gonadal axis which typically allows for the release of follicle-stimulating hormone and luteinizing hormone from the anterior pituitary[36]. The disruption of this process can prevent successful production of both sperm and eggs, resulting in decreased fertility[37].

1.4.3 Anti-depressant

Analysis of CSF and serum from patients with depression have showed a significant decrease in VGF peptide levels, generating new interest into VGF and its secreted peptides and their functionality in the pathology of depression[38,39]. Complementary evidence has shown that after anti-depressant treatment with escitalopram and duloxetine, two common antidepressants, VGF levels were recovered[38]. The restoration of VGF expression post-treatment suggested that VGF and its derived peptides play a functional role in the mechanisms underlying the action of antidepressants and their effects.

One hypothesized mechanism for altered VGF expression upon antidepressant administration suggests that activity-dependent genes like VGF and BDNF have ant-/agonist effects on glutamate receptors such as NMDAR and are upregulated upon antidepressant treatment in a bidirectional manner[40]. Sequentially, upon upregulation of VGF levels in patients with depression, there is a rapid phosphorylation of TrkB and mTOR signaling pathways, allowing for the insertion of GluA1 into the AMPA receptor, which results in downstream antidepressant effects along with secretion of BDNF and VGF, participating in an autoregulatory feedback loop[40,41,42].

1.4.4 Neuroprotection

Biological processes aimed at protecting the nervous system from damage and degeneration, whether it be due to acute or chronic health conditions provide neuroprotection[43]. A large number of signalling pathways are involved in these processes in an attempt to reduce inflammation, apoptosis, and endoplasmic reticulum and oxidative stress[44,45,46]. Some neuroprotective agents have the ability to control these processes, which can reduce the amount of damage inflicted on the nervous system. The poor translational ability of previous neuroprotective agents to transition between animal models and humans suggests that more investigation into promising targets is necessary[47].

Throughout periods of brain damage and dysfunction, such as the progressive course of amyotrophic lateral sclerosis (ALS), it has been shown that VGF expression is also altered suggesting that it could play a role in neurological function and repair[48]. A common source of neurological dysregulation is endoplasmic reticulum (ER) stress, when the ER is unable to properly package proteins due to oversaturation[49,50]. Recent *in vitro* studies looking into ER stress and possible neuroprotective agents has identified VGF as a potential candidate[51]. The small molecule SUN N8075, a known-inducer of VGF expression was used in the Sod1-ALS mouse model. The Sod1-ALS mice are under constant ER-stress resulting in muscle deterioration and early postnatal lethality. Peripheral blood and tissue samples from these mutant mice showed significantly reduced levels of VGF compared to wildtype mice. Upon administration of SUN N8075, the levels of VGF increased in SOD1-ALS mutants and disease progression slowed significantly, prolonging their survival[51].

Although inducing full-length VGF expression has resulted in neuroprotective effects in a model of ER stress, the proteolytic nature of VGF begs the question of which peptide is

responsible. Further investigation demonstrated that the C-terminal VGF peptide LQEQ-19 provided neuroprotective effects[52]. In this study, a mouse motor neuron cell line (NSC34) was serum deprived to induce cell death. Pre-treatment of the cells with different VGF peptides was used to assess their neuroprotective capability. In this way, NSC34 cells pre-treated with LQEQ-19 showed significantly less cell death, than those treated with other VGF peptides. Investigation into the mechanism behind these neuroprotective effects highlighted cell survival pathways Akt/PI3K and ERK/MAPK[53]. Inhibition of these pathways *in vitro*, prevented any neuroprotective effects seen upon LQEQ-19 exposure, making it plausible that the VGF-peptide signals through this pathway. Collectively, these findings suggest that VGF and its derived peptides play a significant role in neuroprotection and the subsequent biological responses.

1.4.5 Neuroinflammation

Inflammatory responses that occur within the central nervous system are typically classified as 'neuroinflammation'[54]. Innate immune cells, microglia and astrocytes, are key mediators of neuroinflammation and participate in both beneficial and damaging inflammatory responses[55]. Often, neuroinflammation is also a mediator of repair processes such as pathogen clearance after a brain injury, facilitating improved functional recovery[56,57]. The delicate balance between the beneficial and detrimental effects of neuroinflammation along with its context-specific nature is crucial to neurological recovery and repair. Identifying key influencers of these processes and optimizing the beneficial effects of neuroinflammation while preventing the detrimental consequences during times of injury and disease is necessary.

One key mediator of neuroinflammatory processes is the complement system and its signalling pathways[58,59]. The complement system is comprised of complement proteins and their

receptors that are capable of altering nervous system pathologies such as recovery after post-traumatic brain injury. C3a, a key mediator of the complement system, signals through its receptor C3aR leading to the activation, survival, and chemotaxis of T-cells and macrophages[60,61]. Recent evidence suggests that C3aR expression on neuronal cells, microglia and macrophages increases during times of neurological stress, such as multiple sclerosis or following stroke. However, the C3a/C3aR signalling pathway has been associated with both beneficial and detrimental effects[62] and previous attempts to control the activation/inhibition of the C3a pathway and its effects have been unsuccessful. In a mouse model of stroke, C3a derived therapeutics were administered during the post-stroke acute phase, resulting in unexpected side effects such as post-reperfusion secondary injury, likely due to the anaphylatoxin properties of C3a[63]. However, when administered after the acute-phase, C3a promotes the clearance of pathogens and debris from the damaged portion of the brain thereby facilitating a faster recovery[58,63].

As discussed above, TLQP-21 signals through C3aR, and participates in complement signaling pathways. However, current evidence has not shown any association between TLQP-21 signaling and the negative anaphylatoxic effects typical of C3a signaling, suggesting that it may be a good candidate for modulating the complement signaling cascade. Recent findings have assessed C3aR signaling and its ability to promote damage and repair in a *Smarca5* mutant mouse model of developmental brain damage[64]. Transcriptomic and histological analysis has shown that VGF may be a key mediator of pathogen clearance, through the TLQP-21/C3aR signaling pathway on microglia, the resident macrophage population of the central nervous system[65]. It is believed that this response activates the merTK pathway, commonly known for its role in the clearance of apoptotic cells[64]. Through the promotion of pathogen clearance and

removal of damaged cells, neuroinflammation can be regulated during times of nervous system damage.

The ability of TLQP-21 to modulate microglial activity in murine models, has been shown to function similarly in human models[66]. When treated with TLQP-21, the murine microglial cell line, BV2, demonstrates increased phagocytic activity and motility, while C3aR1-null murine microglia show impaired phagocytic capacity. Transcriptomic analysis shows overlapping changes induced by both TLQP-21 and C3a super agonist treatment, mainly linked to proliferation and cell migration. Similar activation of phagocytic activity and increased motility is seen in the human microglial cell line, HMC3, upon treatment with TLQP-21, indicating that the biological effects of VGF-derived peptide TLQP-21 is highly conserved among species[66].

1.4.6 Neuropathic pain

Neuropathic pain, a common condition affecting ~8% of the population, often caused by a lesion or disease that affects the somatosensory system, resulting in nerve injury[67]. Alterations in ion channels coupled with alterations in excitatory and inhibitory signalling distort the transmission and modulation of pain signals to the central nervous system[68]. Recent microarray evidence investigating mouse models of neuropathic pain have identified the VGF-peptide TLQP-21 as a major contributor to chronic neuropathic pain[69]. After peripheral nerve injury, the expression of VGF secreted peptides has been shown to increase rapidly in sensory neurons[70]. Recent evidence has also shown that upon intrathecal administration, TLQP-21 has the ability to potentiate neural activity, generating an enhanced pain response[69]. Investigation into the mechanism behind TLQP-21 and neuropathic pain has shown that introducing VGF in models of neuropathic pain

evokes thermal hyperalgesia lasting nearly 120 minutes, while the absence of VGF resulted in a significantly lower level of hypersensitivity. It is hypothesized, that these biological effects are a result of TLQP-21 signaling through its receptor C3aR on the surface of spinal neurons, activating downstream pathways involved in neural signaling[69,71].

1.5 Identification of VGF as a biomarker

Biological compounds referred to as "biomarkers", are used as a measurable indicator of a previously characterized condition or biological process[72]. Typically, these molecules are classified into several categories such as proteins, hormones, cells, molecules or enzymes that indicate a normal or diseased biological state. Biological samples of blood, tissue, exosomes and cerebral spinal fluid (CSF) are used to determine the concentration of these markers in patients with a suspected condition. Observed concentrations are compared to predetermined reference values indicative of a health and/or diseased state. The involvement of VGF in a large variety of biological processes, supported by the characteristics seen in gain/loss of function mouse models of VGF, and its activity-dependent nature suggest that it could be a good biomarker candidate[48,73,74].

1.5.1 Alzheimer's disease

Alzheimer's disease is one of the most common causes of dementia, typically characterized as a neurodegenerative disease causing progressive impairment of cognitive function. The cognitive decline in memory, language, judgement, reasoning and attention is due to the accumulation of amyloid-β and phosphorylated-tau (p-tau) in the brain along with hippocampal atrophy and alterations in brain metabolism[75]. Diagnosis for this condition typically occurs after symptom

onset, but current research has identified multiple biomarkers indicative of Alzheimer's disease. These biomarkers may be able to diagnose patients earlier, determine their prognosis and properly identify candidates eligible for new treatments and clinical trials. Peripheral samples of cerebral spinal fluid and plasma from patients with Alzheimer's disease have consistently shown significantly altered levels of VGF, compared to healthy individuals[76]. One of the largest quantitative proteome studies in patients with Alzheimer's disease to date, identified several altered proteins including VGF in the CSF of Alzheimer's patients using high resolution mass spectrometry. In this regard, VGF was significantly decreased in Alzheimer's patients when compared to healthy controls, identifying it as a novel biomarker for early detection[76].

Further investigation tested the ability of VGF-derived biomarkers to identify patients showing early signs of cognitive impairment, and their ability to predict the conversion from a mild cognitive impairment to Alzheimer's disease[74]. Typically, mild cognitive impairment (MCI) is diagnosed when patients demonstrate measurable levels of cognitive impairment that does not yet meet the threshold for dementia[77]. Patients with this condition are at an increased risk of developing Alzheimer's and current pathophysiology of the MCI to AD transition is poorly understood[77]. Current evidence has identified N-terminal VGF peptide, NSEP-17 (**Figure 2**), as a noteworthy biomarker in MCI patients with suspected AD[74]. NSEP-17 levels were shown to be significantly decreased in the cerebral spinal fluid of these patients, which gives plausible indication of this MCI to AD conversion. A combination approach to diagnosing MCI patients most likely to develop AD using well-characterized biomarkers amyloid β-42 and p-tau coupled with levels of VGF peptides such as NSEP-17, outperformed the conventional biomarkers alone[77].

1.5.2 Amyotrophic Lateral Sclerosis

Amyotrophic lateral sclerosis (ALS) is classified as a progressive neurodegenerative disorder that affects motor neurons responsible for voluntary muscle movement and coordination[78]. There are two main types of ALS, sporadic which is attributed to 90% of cases and familial that accounts for 10%, occurring in patients with specific mutations in over 20 different causative genes. Current evidence suggests that ALS etiology is primarily rooted in oxidative and endoplasmic reticulum stress, protein aggregation, neuroinflammation and altered RNA metabolism[79,80,81]. ALS is predominantly diagnosed by a patient's symptoms and clinical presentation, but it is often misdiagnosed due to a wide variety of clinical features[82]. More recent evidence indicates several biomarkers indicative of ALS pathology, greatly improving current diagnostic measures. Previous evidence from Pasinetti *et al*. looking for biomarkers in the cerebral spinal fluid of ALS patients identified a significant reduction of VGF derived peptide VGF.4.8 (**Figure 2**) (VGEEDEEAAEAEAEAEEAER) with over 97% specificity, 91% sensitivity and 95% accuracy[83]. This biomarker coupled with clinical presentation, provides a more effective diagnosis then any single method alone[83].

Further investigation assessed the ability of VGF to predict ALS before symptom onset using transgenic mouse models with a SOD-1 G93A mutation that present with an ALS phenotype at postnasal day 90 (P90) and complete paralysis by P130[48]. The investigators found that by P75, 15 days before symptom onset, there was a significant decrease in the amount of full-length VGF in the CSF of these mice. Levels of VGF continued to decrease throughout disease progression indicated by muscle weakness and poor behavioral performance. VGF shows promise as an accurate indicator of disease onset and progression, which allows for an earlier

diagnosis and treatment for patients with ALS and it is postulated whether restoring levels of VGF in patients back to baseline levels, could slow the progression of muscle weakness[48].

1.5.3 Neuropsychiatric Disorders

Neuropsychiatric disorders present with patterns of abnormal emotions, behaviours and thoughts that disrupt normal daily living and result in functional impairments and distress[84]. Major depressive disorder (MDD), characterized as having a depressed mood, loss of interest and impairment of cognitive functioning, is one of the most common neuropsychiatric disorders affecting over 264 million people globally[85]. Diagnosing MDD proves difficult, with clinical presentation of symptoms being the main indication, symptoms that overlap significantly with a wide variety of other neuropsychiatric disorders. The high prevalence of MDD along with its limited response rate to therapeutics results in a success rate of less than 30%[38].

The most common therapeutic treatment for MDD is antidepressants, that function through several mechanisms, one of which results in an upregulation of brain-derived neurotrophic factor (BDNF), specifically in the hippocampal region[86]. Variants within the BDNF gene, including a missense mutation (p.M66V) at position 66, result in significantly decreased activity-dependent secretion of BDNF along with reduced hippocampal volume and increased susceptibility to depressive behavior[87,88,89]. Naturally, the robust influence of BDNF on the expression of VGF is greatly impacted in patients and mouse models of depression, with post-mortem examination indicating a significant decrease of both VGF and BDNF in the hippocampal region[38]. Previous attempts to harness the activity-dependent nature of BDNF-VGF have proven successful in mouse models of depression treated with exercise, increasing levels of both BDNF and VGF and reducing depressive behaviours[90].

Due to its similarity to MDD, bipolar disorder (BD) is often misdiagnosed[91]. MDD and BD both present similarly, with extreme fluctuations in energy levels and mood states making it hard to distinguish between the two neuropsychiatric disorders[91]. In an attempt to find biological markers distinguishing between the two disorders, enzyme-linked immunosorbent assays (ELISAs) detected significantly decreased levels of VGF in MDD patients, while patients with BD had slightly higher levels of VGF compared to healthy controls. This distinction between the two disorders is highlighted by tissue analysis in murine models of MDD and BD, showing reduced levels of VGF in mice with depressive behaviors while mice with BD have slightly elevated levels[26,42]. Although the exact mechanism that distinguished between these two neuropsychiatric disorders is not yet known, it is proposed that a decrease in VGF alters synaptic plasticity due to a disruption in the TrkB/mTOR/BICC1 signaling pathway, which is heavily reliant on BDNF expression[14]. The involvement of VGF in synaptic plasticity and neuronal development coupled with its activity-dependent nature, make it plausible to assume that it is involved in the etiology of multiple neuropsychiatric disorders and may have the ability to distinguish between them.

1.6 Stroke

1.6.1 Etiology and physiological responses

Stroke is one of the largest causes of death and disability world-wide, occurring in 10% of those aged 65 years or older making it the third leading cause of death in Canada[92]. Typically, strokes are classified into two main categories, hemorrhagic which is the result of a burst blood vessel or, ischemic which is caused by a clot or thrombotic event that impairs blood flow[93]. When normal blood flow is obstructed to a portion of the brain, cell death occurs generating a

devastating neural event that initiates a cascade of biological processes such as neuroinflammation and oligodendrogenesis[94].

1.6.2 Current treatments

Present treatment options for stroke are very limited, with the only proven effective therapeutic being tissue plasminogen activator (tPA) that functions as an enzyme, promoting the conversion of plasminogen to plasmin, a key mediator of clot breakdown[95]. Although tPA is quite effective, it has significant limitations which contribute to its poor efficacy in most stroke cases. Due to the inherent nature of tPA to breakdown blood clots, it can be catastrophic if administered to someone with a hemorrhagic stroke, resulting in more significant damage and loss of oxygenated blood[96]. The narrow therapeutic time window of tPA is just 4.5 hours, with only ~3.8% of stroke patients receiving the drug in time. This poor efficacy of neuroprotective drugs has shifted the focus of stroke research towards the post-stroke recovery phase in an attempt to optimize neurological processes, promoting repair and regeneration.

1.6.3 Post-stroke recovery phase

Immediately after stroke, the brain is in a state of shock and dysregulation with periods of cell death and inflammation. In an attempt to help minimize damage, the brain initiates three main processes; neurogenesis, the production of newborn neurons; oligodendrogenesis, the production of oligodendrocytes; and inflammation. The extent to which these adult-generated neural precursor cells are able to repair and/or integrate into the damaged portion of the brain is yet to be determined, but early evidence suggests that they may play a supporting functional role[97]. A small subset of these newly generated cells migrate from the subventricular zone towards the

infarct region, integrate into the cortex, and have been shown to have GABAergic properties[97]. These cells have the ability to fire action potentials, exhibit voltage-dependant conductances and express GABAergic markers, VGAT, GAD65 and GAD67. Although these cells are able to integrate into the infarct region, the small number of cells along with their limited ability to receive GABAergic synaptic input greatly reduce their impact on post-stroke recovery[97].

The generation of myelin producing cells after stroke is a crucial part of the post-stroke recovery phase. After stroke, oligodendrocytes in the infarct region are destroyed and new myelin producing cells are required for the brain repair process to begin[98,99]. A portion of the neural progenitor cells in the subventricular zone post-ischemia give rise to non-myelinating oligodendrocyte progenitor cells (OPCs) that later turn into myelin-producing oligodendrocytes[100,101,102,103]. Preclinical results have demonstrated the reparative effects of promoting oligodendrogenesis and the production of myelin-producing cells post-ischemia using pharmacological therapeutics and cell-based therapies[104,105,106,107]. Oligodendrocytes are necessary to coat sprouting axons in myelin sheaths during the post-stroke recovery phase, assisting in the repair and reintegration of the neural network[104].

During times of damage, the body elicits an immune system response, recruiting mediators of inflammation in an attempt to rid itself of pathogens and establish homeostasis. The immediate inflammatory response post-ischemia is localized to the damaged blood vessels and tissues, but is soon propagated through an inflammatory cascade, eliciting a systemic response[108]. This inflammatory response plays an important role in the preservation of neurons and overall recovery post-ischemia, while also potentially exacerbating the tissue injury[109]. The effects of inflammation are seen for days, weeks and months after the ischemic event playing a dual role of damage and repair. Key mediators of this immune response are microglia, the

resident macrophage of the central nervous system[110]. The activity of these cells is largely influenced by signalling cascades from ischemic events, playing both beneficial and detrimental roles in brain repair. Regulation of the inflammatory-autophagy pathway post-stroke functions to inhibit the negative inflammatory effects caused by ischemic damage and assists in re-establishing homeostasis[109]. Upon ischemic stroke, autophagy appears to be activated in glial cells and neurons, resulting in clearance of pathogens and damaged cells in the ischemic region promoting brain repair and recovery[111]. Collectively, these processes mediate the post-stroke recovery phase, exhibiting both beneficial and detrimental effects on brain repair, ultimately setting the stage for long-term recovery.

1.6.4. VGF in the context of stroke

In the acute stages of the post-stroke recovery phase, a period of reorganization and neural regeneration, the brain undergoes many biological processes as previously discussed in **section 1.6.3.** with an increase in the expression of many genes responsible for neural differentiation, synaptogenesis and plasticity. Photothrombosis utilizes a photosensitive dye (Rose Bengal) that promotes platelet aggregation after laser treatment and has been used regularly as a rodent model of ischemic stroke. In this way, the generated lesions are more consistent from experiment to experiment and can be localized to specific regions of the cerebral cortex (eg. Motor cortex).

Using a photothrombotic stroke model in adult mice and analyzing RNA expression in the cortical region surrounding the lesion at seven days post-stroke, VGF was identified as an upregulated transcript[112]. It was postulated that this acute increase in VGF transcript during this period of brain repair could be indicative of its protective and reparative nature[112]. One proposed mechanistic pathway is the cAMP response element in the promoter region of VGF and its

ability to activate cell survival pathways. Complementary findings have demonstrated that the phosphorylation of the ERK/MAPK and Akt/PI3K cell survival pathways lead to an increase in VGF expression, indicative of a mutually-dependent CREB-mediated cycle between VGF and these pathways[113,114].

Furthermore, an *in vitro* model of ischemia in PC12 cells pretreated with full-length VGF peptide was used to assess viability under ischemic stress[112]. Compared to mock controls, VGF-treated cells showed a significant reduction in cell death upon exposure to ischemic conditions. Earlier findings using NGF-treated PC12 cells have demonstrated that VGF is upregulated by a wide variety of growth factors, as mentioned in **section 1.2.1**[4]. Taken together, these findings indicate that neurotrophic factors in the post-ischemic brain may upregulate the expression of VGF transcript levels, promoting enhanced brain repair and stimulating post-stroke recovery processes.

1.7 Rationale, Hypothesis and Specific Aims

Our group has previously demonstrated that the neuropeptide VGF and its derived peptides have the ability to influence the proliferation of oligodendrocyte progenitor cells in a model of developmental brain damage[12]. In this model, conditional removal of the chromatin remodelling protein, Snf2h, results in massive loss of cerebellar granule neurons leading to a disorganized and undersized cerebellum resulting in early lethality. Upon ectopic delivery of adenoviral VGF, the mice showed significantly lengthened survival and an increase in the proliferation of oligodendrocyte progenitor cells, promoting increased myelination. Overwhelming evidence from our group complements previous findings indicating the importance of VGF in neurological disorders and proper neurological functioning. These findings along with the acute upregulation

of VGF expression post-stroke have allowed us to **hypothesize** that VGF and its secreted peptides may activate neurotrophic factors and cell survival signaling pathways in the peri-infarct region post-stroke, thus promoting migration of neural stem cells and immune system response cells, which ultimately result in the clearance of damaged tissue and improved functional recovery. To this end, we have defined three specific aims to explore this hypothesis:

1. Determine the requirement of VGF in post-stroke recovery
2. Examine the effects of exogenous overexpression of VGF and its influence on post-stroke recovery.
3. Determine the effects of VGF on the post-stroke immune response

2. Materials and Methods

2.1 General Mouse Work

2.1.1 Animal Husbandry

Mice were housed at the University of Ottawa's Animal Care and Veterinary Services facility. All experiments and procedures using mice complied with the Ontario Animals for Research Act and were approved by the University of Ottawa's Animal Care Committee and the Canadian Council on Animal Care. Mice were housed at 23$_{o}$C with 28% humidity on a 12-hour light-dark cycle with food and water available *ad libitum*. Breeding pairs were set up with one male and two females in each cage and pups were weaned at 21 days post-birth. At 7-weeks, mice were singly housed in preparation for subsequent experiments. 7-week old Wildtype C57BL/6J mice were purchased from Charles River Labs for use at 10 weeks.

2.1.2 Mouse Models

VGF$_{flpflox/flpflox}$ (referred to herein as VGF$_{f/f}$) C57BL/6J mice were generously provided by Dr. L. Cao at the Ohio State University (Columbus, OH USA) and originally generated by Dr. Stephen Salton's laboratory at Icahn School of Medicine, Mount Sinai (New York, USA). The entire VGF coding region is flanked by loxP sites and homozygous mice maintained on a C57BL/6J background displayed no overt phenotype. Nestin-cre mice were generously provided by Ruth Slack, University of Ottawa, and were previously characterized in *Berube et al. 2005*. VGF$_{f/f}$ mice were bred to Nestin-cre mice to generate heterozygous VGF$_{f/+}$;Nestin-cre$_{+/-}$ mice which were then used to generate a tissue specific conditional knock-out mouse model herein referred to as VGF vKO.

2.1.3 Genotyping

Genotyping was performed using small samples of mouse tissue collected at the time of dissection or weaning (21 days postnatal). Genomic DNA (gDNA) was extracted using DNA lysis buffer (22.5 mM NaOH, 0.18 mM EDTA pH 8.0) at 90$_o$C for 60 min. The solution was then neutralized using neutralization buffer (30 mM Tris pH 8.0) and was kept on ice for 15 min. For each sample a PCR reaction was prepared (1X PCR Buffer, 2.5 µL 2.5 mM dNTP, 0.75 µL 50 mM MgCl2, 0.5 µL primers (**Table 1**), 0.25 µL Taq and 1 µL of tissue lysate) and cycled under the following conditions: 94°C for 3 min, 35 PCR cycles (94°C for 20 sec, 60°C for 20 sec, 72°C for 30 sec) and a final cycle at 72°C for 5 min. DNA loading dye (6X) was added to the PCR reactions which were electrophoresed on a 1% agarose gel prepared by melting 1% agarose (Thermo Fisher, cat #16500500) in 125mL 1X TAE using a microwave with 0.01% ethidium bromide added prior to solidifying in a gel cast. Samples were electrophoresed at 90V for 25 min alongside a DNA ladder (Invitrogen, cat # 10787-026) prior to visualization using ultraviolet light (ChemiDoc-It ts2 Imager).

Table 1. Primers used for Genotyping Mouse Tissue Samples

Gene	Primer	Sequence (5'-3')	Denature	Anneal	Elong.
VGF	F	ACG CCG TCA TCC TTT GGC CG	94$_o$C 20sec.	60$_o$C 20sec.	72$_o$C 30sec.
	R	CCG GGG AGT CCT GTG GGG AG			
Cre	F	ATG CTT CTG TCC GTT TGC CG	94$_o$C 20sec.	60$_o$C 20sec.	72$_o$C 30sec.
	R	5'-GGG CGT AGA CAT CTG GGT AG			

2.1.4 Tissue Collection

Mouse tissue was collected at multiple timepoints for downstream analysis using two methods of collection. Brain samples collected for immunofluorescence were generated by euthanizing mice through CO_2 asphyxiation and dissecting out whole brain tissue which was then saturated in a 4% paraformaldehyde solution for 24 hours. After brains were preserved in PFA, samples were stored in PBS+0.04% sodium azide until utilized. Samples that were obtained for protein or transcript analysis were also collected through CO_2 asphyxiation and dissection of whole brain tissue. Brain samples were then flash frozen in liquid nitrogen and placed in -80^{o}C storage until needed for further processing.

2.2 Photothrombotic Stroke Model

2.2.1 Photothrombosis

Ischemic stroke was induced in the right sensorimotor cortex of mice using a previously described protocol for photothrombosis[115]. Mice were anesthetized with 5% isofluorane and 1% oxygen and placed on a heating pad to maintain body temperature at 37^{o}C which was monitored using a rectal thermometer (Harvard apparatus). The mice were intraperitoneally injected with Rose Bengal Dye (10 mg/ml, 198250-5G; Sigma Aldrich) and were transferred to a stereotaxic frame. A small incision was made to expose the skull. The stroke coordinates (+0.7 anterior-posterior, +1.5 medial-lateral, 3cm laser height) were measured relative to Bregma and five minutes post-injection, a green laser (532nm, 20mW, MGM-20; Beta Electronics) was used to illuminate the brain for ten minutes. The scalp was then closed with tissue glue and 2% transdermal bupivacaine was administered as an analgesic immediately after and again four hours post-surgery along with visual wellness checks.

2.2.2 Infarct volume quantification

Magnetic Resonance Imaging (MRI) was performed on a group of mice 24 hours post-photothrombosis to determine infarct volume. Mice were anesthetized with 4% isofluorane and then maintained with 2% isofluorane for 10-15 minutes while scans were generated using a small-animal scanner (7T General Electric/Agilent MR901). Cardiovascular and respiratory function was monitored throughout the procedure. After the infarct region was located through a preliminary scan, T2-weighted structural images were obtained (15 transverse slices; thickness = 800μm). MRI images were analyzed using the Fiji program[116], and cortical damage was manually traced and measured individually in each slice. Infarct volume was then calculated by multiplying the sum of traced areas in each slice by the slice thickness (0.8mm).

2.3 Adenoviral construction and delivery

2.3.1 Adenoviral Construction

The generation of VGF and control Adenoviruses were described previously in *Alvarez-Saavedra et al 2016*[12].

2.3.2 Intravenous Delivery of Adenovirus

Adenovirus expressing VGF or an empty control was diluted in PBS to 1 x 10^{12} viral particles per kilogram in a final volume of 100 μL and intravenously injected into mice 48 hours post-photothrombosis through tail-vein injection.

2.4 Behavioural Analysis

Behavioural testing was performed to evaluate sensorimotor function in mice pre- and post-impairment of the right forelimb after inducing ischemic stroke in the left sensorimotor cortex.

The mice were singly housed under normal conditions with a 12-hour light cycle (7am-7pm). When appropriate, training for the behavioural test was done prior to the start of the experiment. Atleast 10 mice were used for each behavioural experiment, while numbers ranged from 8-15 mice per group depending on availability.

2.4.1 Cylinder Test

The cylinder test was used to assess spontaneous forelimb function in mice pre- and post-photothrombosis[117,118]. The mouse is placed into a 10 x15 cm glass beaker and was observed under red light for a minimum of 20 rears [places its forelimbs on the side of the cylinder]. The mouse was recorded using Ethovision XT 11 and the videos were scored blind to genotype for the amount of time spent on each forelimb and quantified. Percentage of time spent on the right forelimb was calculated using the following formula: [(Time on right forelimb)/(Time on right forelimb + Time on left forelimb)]*100.

2.4.2 Horizontal Ladder

The horizontal ladder test was performed using a protocol previously established by Farr T. *et al*., 2006[119]. The test was used to assess forelimb function of mice pre- and post-photothrombosis. Training for the test was performed several days before photothrombosis and baseline performance was established. Mice were trained over two consecutive days, performing 4-5 training trials per day. The test was performed using a plexiglass ladder (69.5 cm x 15 cm) with metal rungs irregularly spaced that was elevated using a clean cage on one side and their home cage on the other. Mice were video recorded as they crossed the ladder [unassisted] 3 consecutive times per timepoint and the last two trials were hand-scored. The recorded videos

were blinded to genotype and analyzed at 0.12x speed to examine forelimb placement, noting the number of 'successful steps', 'missteps' (foot faults) where the mouse did not grasp the ladder rung, as well as 'cheats' where the mouse used the walls of the apparatus for support to cross the ladder. Percentage of error was calculated for each subject using the following formula: [(Missed steps)/(Sucessful steps + missed steps + cheats)]*100.

2.5 Immunostaining and counting

2.5.1 Transcardial Perfusion and Fixation

Anesthetized adult mice were perfused with 20 mL of phosphate buffered saline (PBS) followed by 20mL of 4% paraformaldehyde (PFA, pH 7.4) (P-6148, Sigma) injected transcardially into the left ventricle. Brains were then dissected and placed in 4% PFA overnight at 4^{o}C and then cryoprotected in 30% sucrose (0.1% sodium azide (NaN_3 – S2002, Sigma, in 1X PBS) for at least 48 hours at 4^{o}C.

2.5.2 Immunofluorescence

After transcardial perfusion and fixation (**Section 2.5.1**), brains were sectioned using a microtome (SM 2010R; Leica) at a thickness of 40µm. Serial sections were placed into nine wells of a 12-well plate containing 1X PBS with 0.1% NaN_3 and were stored until staining. Free-floating sections were then removed from the wells and washed three times in 1X sterile PBS and then placed into sodium citrate (pH 6) antigen retrieval solution (if deemed necessary) in a 12-well plate which was then placed in an 80^{o}C incubator (Hybaid Shake n' Stack, ThermoFisher) for 30 minutes and then allowed to cool to room temperature. After antigen retrieval, sections were washed 3 times in 1X PBS and placed into a blocking solution (10%

horse serum, 0.1% Triton X-100, 0.1% Tween-20 in 1X PBS) for one hour at room temperature. Sections were then incubated in primary antibody (**Table 2**) in a PBS solution (0.04% Triton X-100, 3 mg/mL bovine serum albumin in 1X PBS) overnight at 4$_{o}$C. Sections were then washed in 1X PBS three times before being incubated in the appropriate Alexa Fluor® (Jackson Immunoresearch) secondary antibody diluted 1:500 in PBS and incubated for one hour at room temperature. Next, sections were then washed in 1X PBS three times, incubated in Hoechst stain (62249, ThermoFisher) for 10 min at room temperature and then washed twice in 1X PBS. Free floating sections were then mounted onto SuperFrost Plus slides (Fisher, 12-550-15) using immunomounting solution (S3023, Agilent Tech.) and coverslips.

Table 2. Primary antibodies used for immunofluorescence and immunoblotting

Antibody	Species	Manufacturer	Immunofluorescence dilution	Immunoblotting dilution
Akt	Ms	Santa Cruz (sc81434)	-	1:250
p-AKt	Ms	Santa Cruz (sc-514032)	-	1:500
ERK	Rb	Santa Cruz (sc154)	-	1:2000
pERK	Ms	Santa Cruz (sc7383)	-	1:250
GFAP	Ms	Santa Cruz (sc65343)	1:1000	-
VGF (R15)	Gt	Santa Cruz (sc10383)	1:100	-
VGF	Rb	Cedarlane (custom Ab)	-	1:500
Iba1	Rb	Wako (019-19741)	1:500	-
Vinculin	Rb	Abcam (ab129002)	-	1:2000
DCX	Gp	Millipore (ab2253)	1:1000	-
Ki67	Rb	Abcam (ab16667)	1:500	-
β-actin	Ms	Sigma (A1978)	-	1:1000

Table 3. Secondary antibodies used for immunofluorescence and immunoblotting

Wavelength	Species	Manufacturer	Immunofluorescence dilution
488	Gp	Invitrogen (A-11073)	1:500
555	Rb	Invitrogen (A-32794)	1:500
594	Rb	Invitrogen (A-32754)	1:500
647	Ms	Invitrogen (A-32787)	1:500

2.5.3 Confocal Microscopy

Images of immunofluorescent sections were acquired using a Zeiss LSM800 AxioObserverZ1 confocal microscope with both 10X and 20X objectives. Emission wavelengths of 488, 555 and 647 were used and images were acquired using optical z-stack sectioning through ZEN 2009 acquisition software (Zeiss). Images were then exported into Adobe Photoshop for organization into final figures.

2.5.4 Cell Counts

Cells in the peri-infarct region were quantified manually using Fiji by an observer blinded to the sample identity[116]. The peri-infarct region was defined by the observer as the area between the cortical infarct and the lateral ventricle.

2.6 Protein Analysis

2.6.1 Protein Isolation

Mice were asphyxiated using CO_2 and immediately decapitated using scissors. The brain was then isolated and removed prior to being suspended into 1 mL protein lysis buffer (150 mM NaCl, 50 mM Tris, 5 mM EDTA, 1% NP40, 0.1% SDS in ddH_2O) supplemented with protease

inhibitor cocktail (Calbiochem, 539134-1SET) on ice. Tissue was sheared using a TissueTearorTM for 45 seconds. For *in* vitro protein experiments, cells were collected and centrifuged to remove any remaining media and were then resuspended in PBS before being centrifuged once more. Cells were then resuspended in protein lysis buffer supplemented with protease inhibitor cocktail as previously described. Lysates were then placed on ice for 15 minutes and were then centrifuged for 10 minutes at 4$_{o}$C at 13,000 RPM (Galaxy 20R Microcentrifuge, VWR). Supernatant was then transferred to a new tube and protein concentration was spectroscopically quantified using Protein Assay Reagent (Bio-Rad, Mississauga, ON) using the manufacturer's instructions with an Eppendorf BioPhotometer. 4X NuPage LDS sample buffer was added to protein lysates (Thermo Fisher, NP0007) and samples were heated to 95$_{O}$C for 5 minutes and then put on ice prior to gel electrophoresis and immunoblotting.

2.6.2 Gel Electrophoresis and Immunoblotting

To assess relative protein expression in the adult mouse brain tissue or collected cell lysate (**Section 2.6.1**), gel electrophoresis and immunoblotting was used to separate proteins by their molecular weight and identify them with antibody staining. Prepared samples were loaded onto 4-12% Bis-Tris pre-cast gels (Invitrogen, NP0321BOX) along with 7 μL of Blueye Prestained Protein Ladder (FroggaBio Inc, cat # PM007-0500) for sodium-dodecylsulfide polyacrylamide gel electrophoresis (SDS-PAGE) at 170V for 80 minutes (XCell, SureLock Mini-Cell, ThermoFisher) in 1X MOPS running buffer (Fisher, BP308-500). The protein was then transferred onto polyvinylidene difluoride (PVDF) membrane (BioRad, cat # 162- 0177) for 70 minutes at 100V in 1X transfer buffer (20% MeOH, 50 mM Tris, 40 mM Glycine). Membranes

were then washed in 1X PBS three times for 10 minutes and blocked with 5% milk and TBS-T solution in tris buffered saline with tween (TBS-T) for one hour at room temperature. The membrane was then incubated in primary antibody in a 5% milk and TBS-T solution (**Table 2**) overnight at 4$_{o}$C and then washed in 1X TBS-T three times for 10 minutes each. Subsequently, the membranes were placed in HRP-conjugated species-specific secondary antibody in a 5% milk solution for one hour at room temperature and then washed in 1X TBS-T three more times before being incubated in ClarityTM Western ECL Blotting Substrate (BioRad, cat # 170-5061) for 5 min. Protein signals were then detected by exposing membranes to film (Harvard Apparatus Canada, DV-E3012).

2.6.3 Protein Quantification

Films with detected protein signals (**Section 2.6.2**) were scanned on a tabletop scanner and saved as .jpg images. The files were then opened in Fiji[116] and measurements of identical areas were taken for each band based on the 'grey mean value'. The relative protein expression was then quantified by subtracting the background signal from the detected protein bands and calculating expression ratios relative to the loading control.

2.7 Cell Migration Assay

2.7.2 RAW264.7 Cell Cultures

The microglia cell line Raw264.7 cells (ATCC, TIB-71), were cultured in complete DMEM (Multicell, 319-005-CL) with 10% fetal bovine serum (FBS, Life Tech., 12483020) and 1% Penn-Strep (Gibco, 15070-063) under incubator conditions of 37$_{o}$C with 5% CO2. When cells reached 75% confluency they were split (3:1) and propagated for a maximum of 6 passages.

2.7.3 Boyden Chamber Migration Assay

Chemotactic properties of VGF were assessed using a 24-well microchemotaxis plate with transwell inserts (VWR, 29442-120) with a polycarbonate filter separating the upper and lower wells (8 μm pore size). Raw264.7 cells (~5x10_4 cells) in 100uL of serum-free DMEM were seeded in the upper well/layer along with any inhibitors, while the lower well/layer contained various peptides diluted in serum-free DMEM. As a gradient control, medium with the same concentration of peptide was added to both the upper and lower wells/layers of multiple inserts. The chamber was then incubated at 37$_o$C with 5% CO_2 for 4 hours. Any remaining cells contained in the upper layer were removed using a cotton swap and the cells in the lower layer were fixed with MeOH for 10 minutes, stained with cresyl violet dye (Fisher, AC405760100) for 30 min, and then rinsed with PBS and mounted onto Superfrost slides (Fisher, 12-550-15). Migration of cells was quantified by counting cells in 10 fields of view of each insert, obtained using a 20X objective on an Axioscope 5 (Zeiss). Images were opened in Fiji[116] and cells were counted manually by an observer blinded to the experimental conditions. 40-80 fields in 4-8 wells for each condition were assessed using cells from 4 different Raw264.7 cell culture experiments.

2.8 RT-qPCR

2.8.1 RNA isolation

Peri-infarct regions were dissected from adult mice post-photothrombosis using a Leica MZ95 stereomicroscope (Meyer). The inner portion of the cortical plug (ischemic lesion) was removed and tissue in adjacent areas between the infarct and lateral ventricle were dissected and placed

into 1mL TRIzol (Life Technologies, cat # 15596018) and RNA isolation was performed as per the manufacturer's instructions. Briefly, chloroform was added to the TRIzol solution and then centrifuged at 12,000 g for 10 minutes at 4^{o}C. The aqueous phase was removed and placed into new tubes containing 500µL isopropanol and 1µL glycogen (Ambion, cat # 9510). The solution was centrifuged again until RNA pelleted. RNA was then washed in 75% ethanol and allowed to air dry at room temperature. Subsequently, 20µL of nuclease-free water was added to the sample and the integrity and concentration of the RNA was quantified using a NanoDrop™ (ThermoFisher, ND-1000) and was then stored at -80^{o}C.

2.8.2 Reverse Transcription

To assess transcript levels, qPCR was performed using complementary DNA (cDNA) generated from isolated RNA (**Section 2.8.1**). cDNA was generated using RNA and random hexamer primers (Thermo Fisher Scientific #SO142) as per the RevertAid Reverse Transcriptase protocol (Thermo Fisher Scientific). Briefly, 5ug of RNA, nuclease-free water and 1µL random hexamer primers (300 ng/µL) were combined for a total volume of 16 µL. The solution was incubated at 70^{o}C for 5 minutes (annealing process) and then placed on ice. Subsequently, 5 µL Revertaid 5X buffer, 1 µL dNTPs (25 mM), 1µL Revertaid enzyme, 0.6 µL RNase out (Invitrogen, AM1906) and 1.4 µL HPLC H_2O were added to each sample. Lastly, the samples were incubated in a thermocycler (Eppendorf, 6321000515) for 5 minutes at 25^{o}C, 1 hour at 42^{o}C and then 70^{o}C for 10 minutes to complete the reverse transcription process and generated cDNA was stored at -20^{o}C.

2.8.3 qPCR

Previously generated cDNA (**Section 2.8.2**) was diluted to 1:10 in nuclease-free H_2O before undergoing qPCR. Reactions for each sample were performed in triplicates and were prepared by mixing 2 µL of cDNA, 10 µL of SensiFAST SYBR Lo-ROX Master Mix (FroggaBio Inc, cat # BIO-94020), 6.4 µL nuclease-free water and 0.8 µL of both the forward and reverse primers (10 nM, **Table 4**). Reactions were loaded into a 96-well plate (Life Technologies, cat # 4346906) and run on an Agilent Stratagene Mx3000P using the following parameters: 95^{o}C for 2 minutes, 40 cycles of (95^{o}C for 5 sec, 60^{o}C for 30 sec, 72^{o}C for 20 sec) and 72^{o}C for 1 minute. The relative transcript levels for each sample were determined using a housekeeping gene (GAPDH) for reference. The fold-change was then calculated using the double delta CT analysis method[120]. Significance was determined using an unpaired students t-test.

Table 4. Primers used for qPCR

Gene	Primer	Sequence (5'-3')
VGF	F	ACGCCGTCATCCTTTGGCCG
	R	CCGGGGAGTCCTGTGGGGAG
C3aR	F	AATGTCCTCACAGCCGCCGTACC
	R	ATCAGCGGTGTCGGCACATGATT
BDNF	F	AGCCTCCTCTTCTCTTTCTGCTGGA
	R	CTTTTGTTGTCTATGCCCCTGCCTT
Iba1	F	AACCTCTCTCAGGGGCTACAG
	R	CTGACGAACACAAACCCAAGTC
GFAP	F	GGTCCCTGTCCTAACCTCCA
	R	AGGAACCCTCCGTTGCTTAC

GAPDH	F	CGGCAAATTCAACGGCACAG
	R	TCACAAACATGGGGGCATCG
MerTK	F	ATCTCACGTGTGGGAAAGCG
	R	GACGAGGGTGCGTAATCTACC

2.9 Statistical Analysis

2.9.1 Prism

Statistical analyses were performed using Prism 6 (GraphPad). When two independent variables were being analyzed, an unpaired t-test was used while dependent groups were analyzed using a paired t-test. Data with two variables were analyzed using a two-way analysis of variance with repeated measures (ANOVA).

3. Results

3.1. VGF plays a key role in the mediation of the post-stroke recovery

3.1.1 VGF:nestin-cre knockout mice show no significant neurological deficits despite decreased body weight.

VGF has been shown to play an interesting role in the maintenance and functioning of the central nervous system. To determine the effects of removing VGF from neuronal cells, we generated a transgenic knockout mouse using a nestin-cre promoter to conditionally ablate VGF from neural progenitor cells (**Figure 4**). The *VGF*$^{fl/fl}$:nestin-Cre$^{+/-}$ conditional knockout (here on called *VGF* cKO) mice showed normal Mendelian ratios and were similar in size to wildtype littermates at birth, but showed significant differences in weight at weaning (P21) with *VGF* cKO mice weighing ~40% less than control littermates (**Figure 4B**). At dissection, adult *VGF* cKO mice had no detectable body fat in their truncal region compared to WT littermates which contributed to their significantly leaner profile and was consistent with previous reports of *VGF* KO mice (**Figure 1A**). Previous studies have demonstrated a difference in brain weight between *VGF* knockout mice and WT[26], As such, we compared the brain weight of *VGF* cKO mice and their WT littermates (**Figure 4C,D**). There was no significant difference in the brain weights of *VGF* cKO and WT mice at weaning and no obvious morphological differences (**Figure 4C,D**).

When assessing the brain-to-body weight ratio (**Figure 4E**), we determined that there was a significant difference between *VGF* cKO mice and their WT counterparts due to the vast difference in body weight, consistent with previous reports of *VGF* knockout mice displaying lean, hypermetabolic phenotypes[21,22]. We did observe a greater variation in the brain-to-body weight ratio in the *VGF* cKO mice compared to WT littermates (**Figure 4E**), which could indicate that these mice are more susceptible to metabolic changes.

3.1.2 Absence of VGF in neural progenitors does not impact neurodevelopment of prenatal and neonatal mice.

The significant difference in body weight between *VGF* cKO mice and their wildtype littermates with little change in brain weight, led us to investigate the neural development of these mice. Over the course of neurodevelopment, the neocortex is generated in an 'inside-out' fashion by an intrinsic genetic program driving the timed differentiation of progenitor cells into diverse neuronal sub-types that migrate to their appropriate layers[121]. Disruption in the formation of these cortical layers can lead to alterations in the growth and functional development of the brain. Using immunohistological analysis in prenatal (E15) and postnatal (P0) transgenic mice, cortical layer markers were quantified in both the transgenic and wildtype mice. Antibodies specific to Pax6 and Tbr2 were used to assess the generation of neural progenitors in E15 mice, identifying the ventricular zone (VZ) and subventricular zone (SVZ) respectively (**Figure 5A,D**). No significant differences were observed in the proportion of neural progenitors in the VZ or SVZ of the *VGF* cKO mice compared to wildtype littermates. We then assessed the development of the cortical layers at P0, using antibodies specific to Tbr1, Ctip2, and Satb2 identifying layers VI, V, and II-IV, respectively (**Figure 5B**). Quantification of the proportion of layer marker positive cells to the total number of cells within the cortex demonstrated that there was no difference between the knockout mice and wildtype littermates (**Figure 5C**). Altogether, these results demonstrate that in the absence of VGF in neural progenitor cells, corticogenesis proceeds normally during brain development.

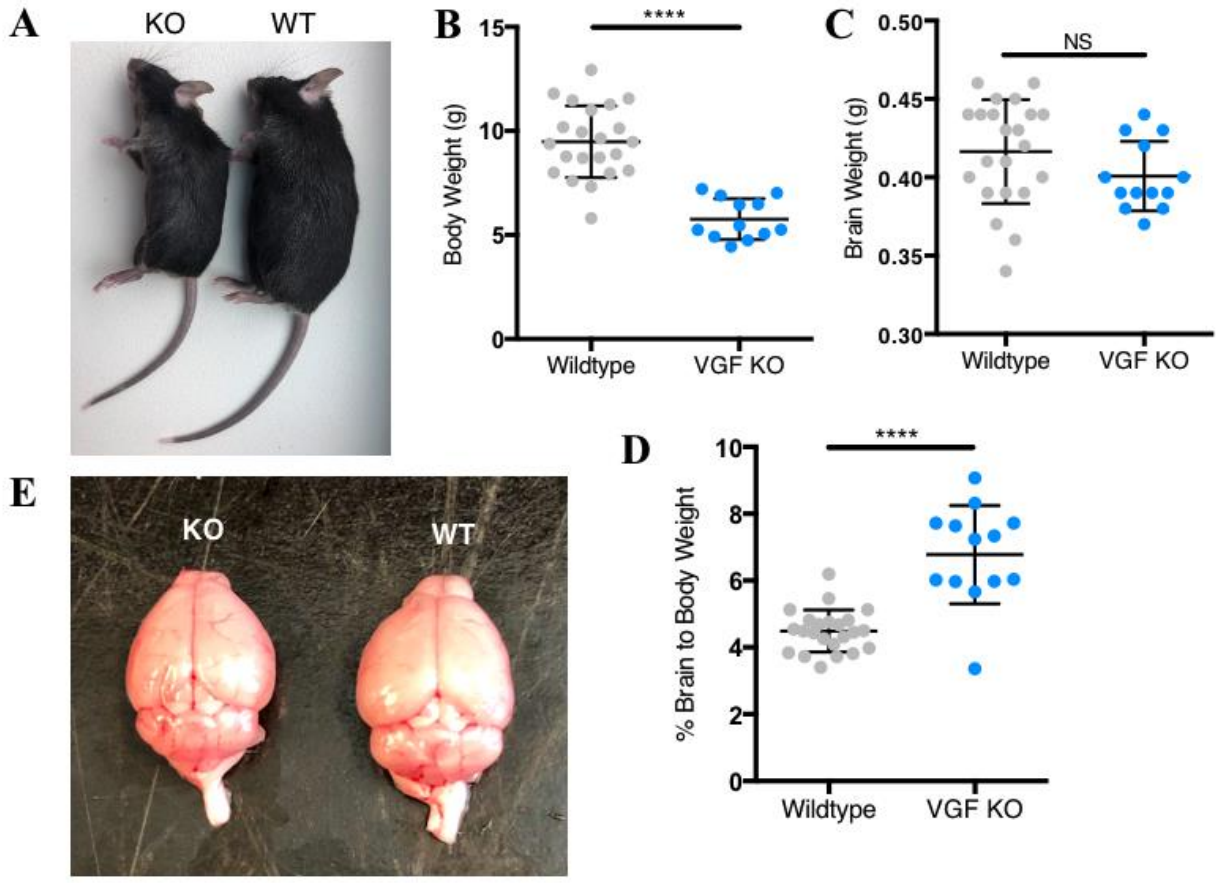

Figure 4. VGF;Nestin-cre knockout mice weigh significantly less than WT littermates. A. Relative size of 21 day old $VGF^{flox/flox}$;Nestin-$cre^{+/-}$ knockout (*VGF* cKO) mice (left) compared to $VGF^{flox/flox}$ littermates (WT; right). B. Quantification of body weight ($t=6.870$, $df=32$, $p<0.0001$) and C. Brain weight ($t=1.504$, $df=33$, $p=0.1422$) of 3-week-old *VGF* cKO knockout mice in comparison to WT littermates. D. Brain to body weight percentage of WT and *VGF* cKO mice.

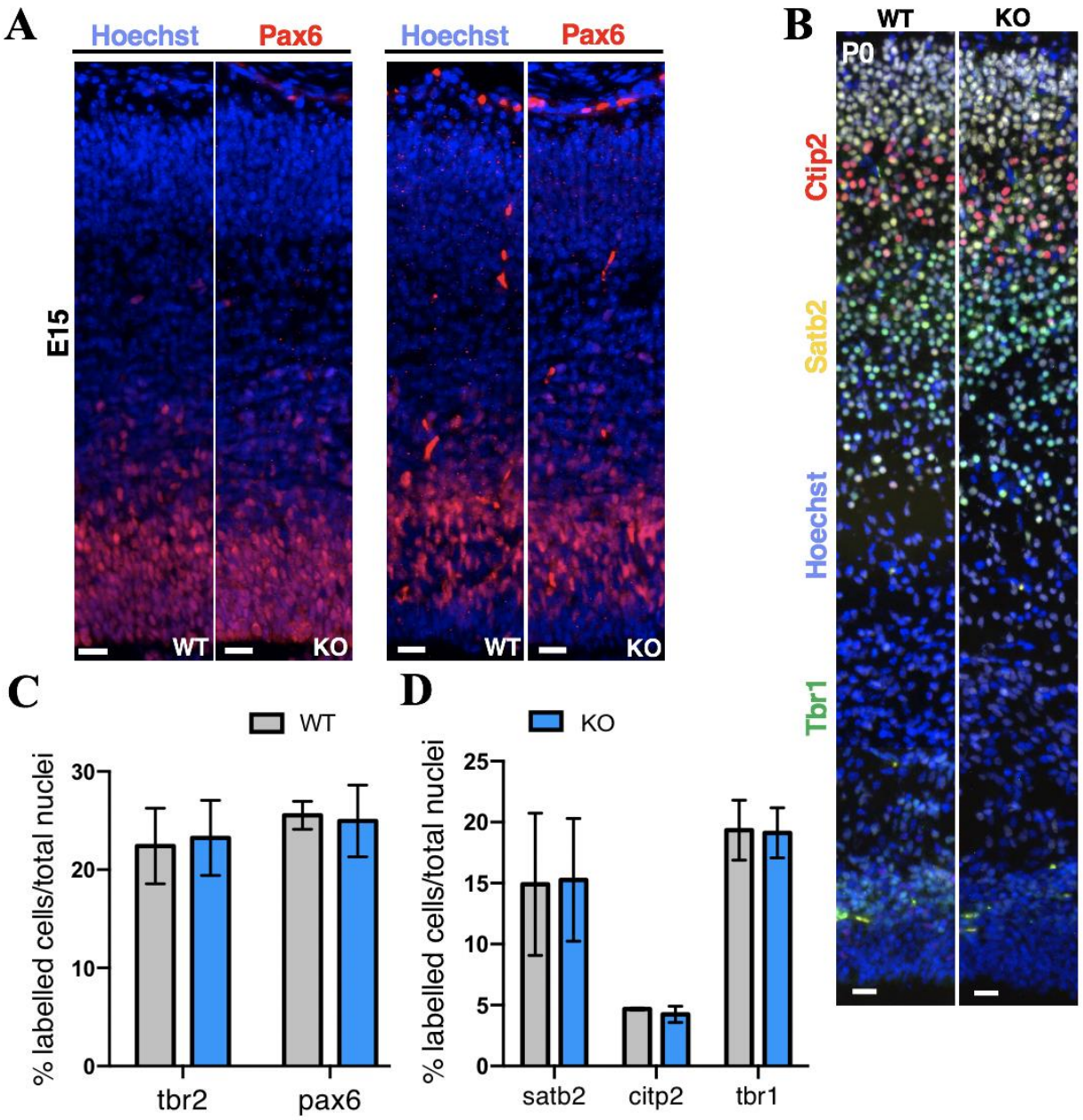

Figure 5. VGF:Nestin-cre knockout mice exhibit normal cortical development. A. Relative size of 8-week-old VGF;Nestin-cre knockout mice (left) compared to $VGF^{flox/flox}$ littermates (right). B. Quantification of body weight ($t=6.870$, $df=32$, $p<0.0001$) and C. Brain weight ($t=1.504$, $df=33$, $p=0.1422$) of 3-week-old VGF;Nestin-cre knockout mice in comparison to $VGF^{flox/flox}$ littermates. D.____ (n=7 WT, 6 KO) E. Immunofluorescent staining of P0 cortical sections from VGF;Nestin-cre knockout mice and $VGF^{flox/flox}$ littermates (WT) labelled with cortical layer markers Tbr1, Satb2, Ctip2, (n=3 WT, 3 KO). Scale bar=10µm. F. Fold Change of VGF and BDNF from RNA isolated from VGF;Nestin-cre knockout mice and $VGF^{flox/flox}$ littermates (WT), determined through qPCR, normalized to housekeeping gene Gapdh ($t=131.36$, $df=4$, $p<0.0001$), (n=3 WT, 3 KO). G. VGF expression assessed using immunoblotting of cortical protein samples from VGF;Nestin-cre knockout mice and $VGF^{flox/flox}$ littermates (WT). Error bars represent standard deviation.

3.1.3 Locomotor analysis of *VGF* cKO mice show no significant difference compared to wildtype littermates.

Prior to assessing stroke deficits within the motor cortex, it was important to determine if there were any pre-existing locomotor deficits in the *VGF* cKO mice that may compound the analysis. To assess the baseline functional capabilities of these mice compared to WT littermates, we performed a beam break assay, a standard locomotor activity test that measures spontaneous activity in the home cage of the mouse over a period of 48 hours[122].

We determined that the total amount of time the *VGF* cKO mice spent moving around their cage over the 48-hour period mirrored that of WT littermates, except at the 44-hour timepoint where the WT mice were more active (**Figure 6A**). This slight reduction of ambulation at a single timepoint when coupled with the rest of the timepoints in the *VGF* cKO mice compared to their WT counterparts is not indicative of gross motor deficits. Similarly, when we examined the total movement time, which includes grooming, eating, and drinking, the knockout mice showed no significant difference over the 48-hour period compared to WT mice, further supporting that they maintain normal gross motor function.

3.1.4 Protein and RNA quantification of *VGF* cKO mice shows significant ablation of VGF in brain tissue.

Nestin-cre transgenic mouse models have historically been used to assess the significance of a specific protein in neural development. This model, as previously mentioned (**Section 2.2.1**), was used to determine the requirement of VGF under ischemic conditions. Firstly, it was imperative to determine whether the transgenic ablation of *VGF* in neural stem cells was effective using the Nestin-cre driven model. Using cortical tissue from 8-week old *VGF* cKO mice and WT littermates, RNA transcript quantification showed that there was a nearly 100%

decrease in VGF knockout mice without a significant change in the levels of BDNF transcripts (**Figure 7A**). This significant reduction of the *VGF* transcript indicates the successful excision of the *VGF* gene in neural progenitor cells, consistent with the known Cre expression pattern of Nestic-cre transgenic mice. Further analysis by immunoblot confirmed the reduction of VGF protein in cortical tissue of 8-week old *VGF* cKO and WT littermates (**Figure 7B**). We observed a complete ablation of VGF protein in the cortical tissue samples of *VGF* cKO mice while WT littermates showed a prominent band at the correct size, thereby confirming the validity of the Cre driver.

3.1.5 Absence of VGF does not affect infarct size post-photothrombosis induced ischemia

Despite that the *VGF* cKO brain was morphologically normal, we wanted to assess whether loss of VGF could impact the size of the infarcted region following phtotothrombotic stroke. Following photothrombosis-induced ischemia in adult mice, MRI analysis was used to determine the infarct volume 24hr post-ischemia (**Figure 8A**). We observed no significant difference in infarct volumes between the *VGF* cKO mice compared to wildtype littermates (**Figure 8B**). We did observe a slightly larger variation in the infarct sizes of *VGF* cKO mice, which was attributed to limitations in the accuracy of laser targeting, coupled with the smaller size of the knockout mice. The lack of any significant differences in infarct size suggested that further studies assessing functional differences could be attributed to the loss of VGF and its effect on the post-stroke recovery phase rather than being attributed to a difference in infarct size.

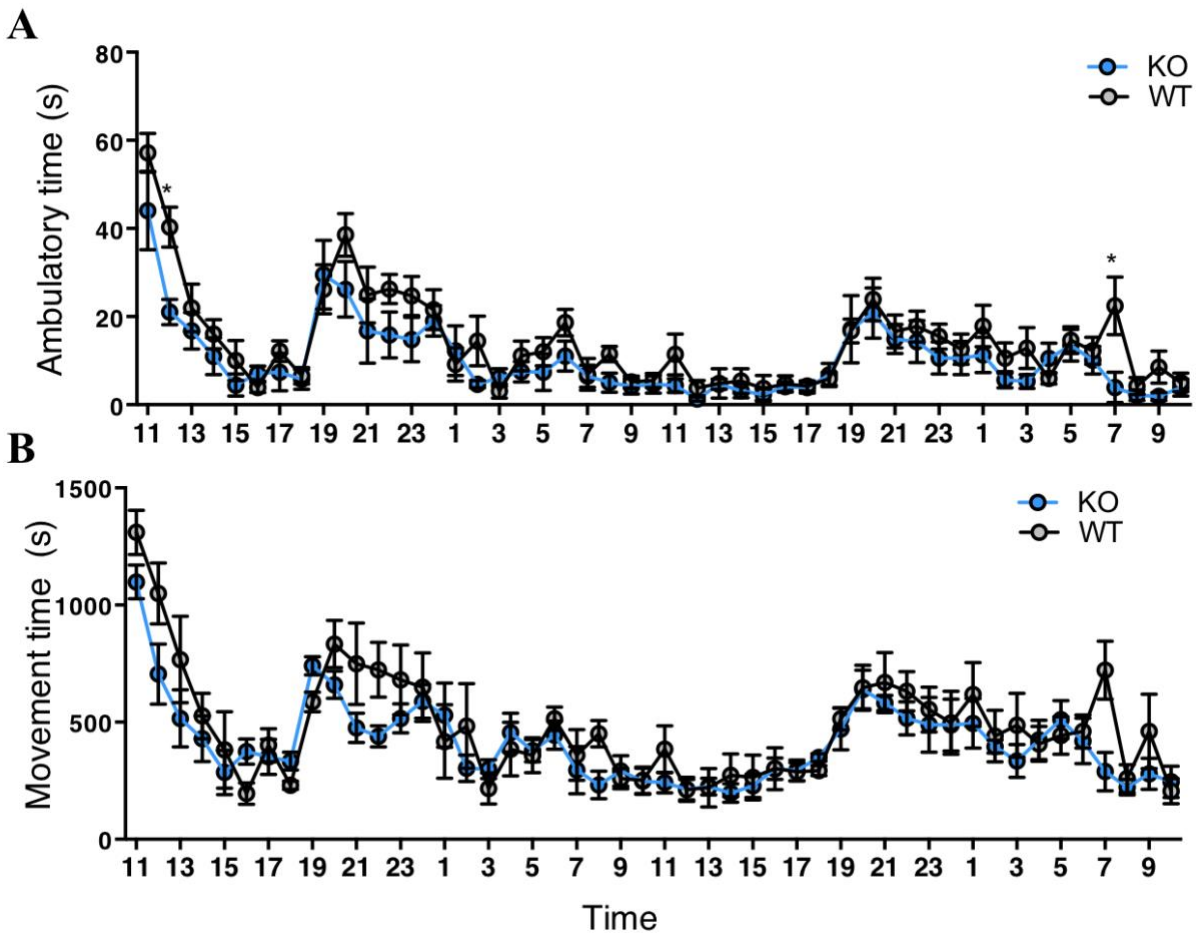

Figure 6. VGF knockout mice show no significant motor deficits compared to WT littermates. A beam break behavioural test on 8-week-old VGF KO mice and WT littermates measuring ambulatory (**A**) and movement (**B**) time over 48 hours (n=6 WT, 7 KO)

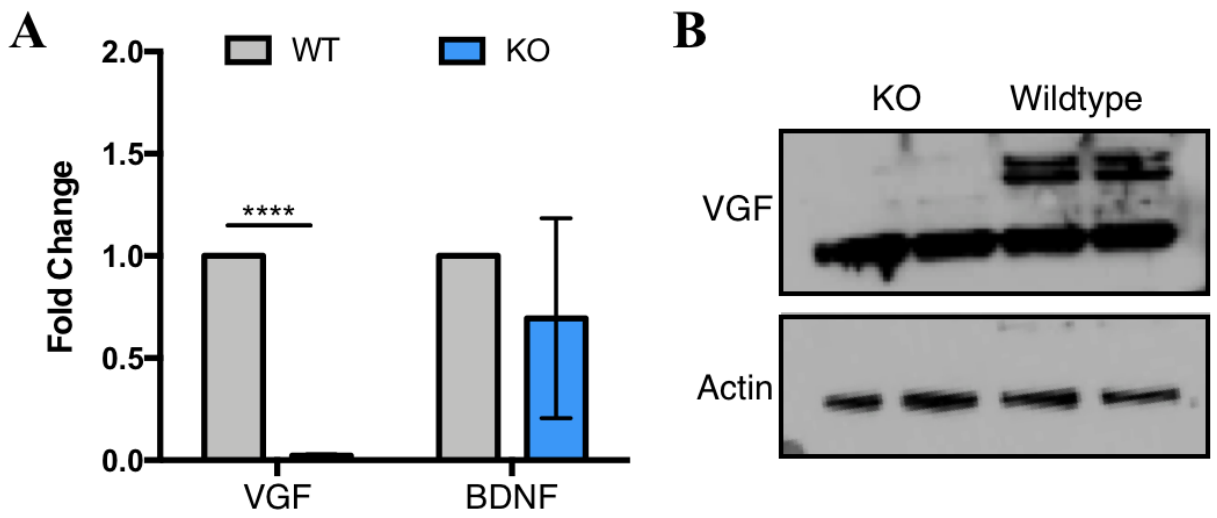

Figure 7. Confirmation of VGF ablation in VGF:Nestin-cre knockout mice. A. Fold Change of VGF and BDNF from RNA isolated from VGF;Nestin-cre knockout mice and $VGF^{flox/flox}$ littermates (WT), determined through qPCR, normalized to housekeeping gene Gapdh ($t=131.36$, $df=4$, $p<0.0001$), (n=3 WT, 3 KO). B. VGF expression assessed using immunoblotting of cortical protein samples from VGF;Nestin-cre knockout mice and $VGF^{flox/flox}$ littermates (WT). Error bars represent standard deviation.

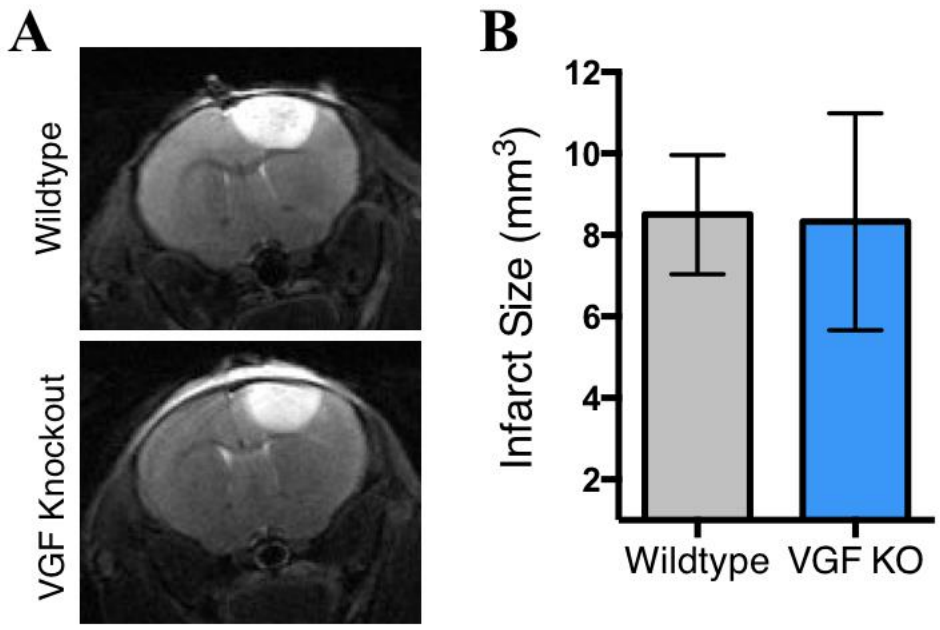

Figure 8. VGF:Nestin-cre knockout mice show no significant difference in volume of peri-infarct region. A. MRI images of VGF;Nestin-cre knockout mice and $VGF_{flox/flox}$ littermates (WT) 24h after photothrombosis, highlighting infarct tissue in cortical region quantified in B. (t=0.1158, df=6, p=0.9116), (n=4 WT, 4 KO).

3.1.6 Absence of VGF in neural progenitor cells significantly affects the post-ischemic migration of neural stem cells in the peri-infarct region.

As previously mentioned (**section 1.6.3**), during the post-ischemic recovery phase there are many processes at work in an effort to re-establish equilibrium and repair the damaged brain. The production of neural stem cells originating from the subventricular zone has long been associated with post-ischemic repair mechanisms and is hypothesized to play a beneficial role in the post-ischemic recovery phase[123]. We sought to assess the histological properties of neural stem cells in the peri-infarct region of mice without the expression of VGF compared to their wildtype littermates. Using 8-week old *VGF* cKO mice and their WT littermates, we induced right-sensorimotor cortical ischemia using photothrombosis and monitored the mice throughout recovery. Immunofluorescent staining of cortical sections from *VGF* cKO mice and WT littermates using DCX, a marker of newborn neurons, was performed at 14 days post-ischemia (**Figure 9A**). We observed that the migration of newborn neurons towards the damaged region of the brain in the *VGF* cKO mice showed a significant reduction in the number of DCX+ cells transiently migrating from the subventricular zone to the outer cortex compared with the WT animals. However, the overall number of newborn neurons in the entire cortical section remained relatively unchanged (**Figure 9B**). It seemed that the newborn neurons in the *VGF* cKO mice were sequestered to the subventricular zone suggesting that VGF promotes the migration of these cells. This finding clearly highlighted the importance of VGF in the post-stroke recovery brain microenvironment.

3.1.7 Mice lacking VGF show significantly reduced behavioural recovery post-stroke compared to wildtype littermates.

Next, we assessed the functional recovery of *VGF* cKO mice and their littermates post-photothrombosis induced ischemia. Similar to the histological experiments, 8-week old adult

mice underwent photothrombosis, inducing ischemia in their left frontal cortex ultimately resulting in right forelimb impairment. The motor function of these mice was assessed at multiple timepoints and compared to their wildtype littermates using multiple behaviour tests. The cylinder test (**section 2.4.1**) is commonly used to evaluate motor function in models of neurological diseases by measuring locomotor asymmetry. Similarly, the horizontal ladder test (**section 2.4.**2) is used to detect changes in motor function in models of neurological disease and impairment, making these suitable choices to evaluate post-stroke performance. Upon testing, it was apparent that the *VGF* cKO mice performed significantly worse in both the cylinder and horizontal ladder behavioural tests (**Figure 10A, B**). In the cylinder test, the *VGF* cKO mice spent significantly less time on their right forelimb compared to wildtype littermates, which indicated that they were favoring their non-impaired hand 11% more than wildtype littermates (**Figure 10A**). The knockout mice also made significantly more errors while completing the horizontal ladder test, with most mice performing close to 9% worse than the wildtype littermates, which was indicative of increased behavioural deficit (**Figure 10B**). The combined results from these two motor function assessments have demonstrated that the *VGF* cKO mice performed worse than wildtype littermates at 1, 14, and 28 days post-ischemia. These findings suggest that there was a larger behavioural deficit in the *VGF* cKO mice post-stroke, which is maintained throughout the first 4 weeks of recovery.

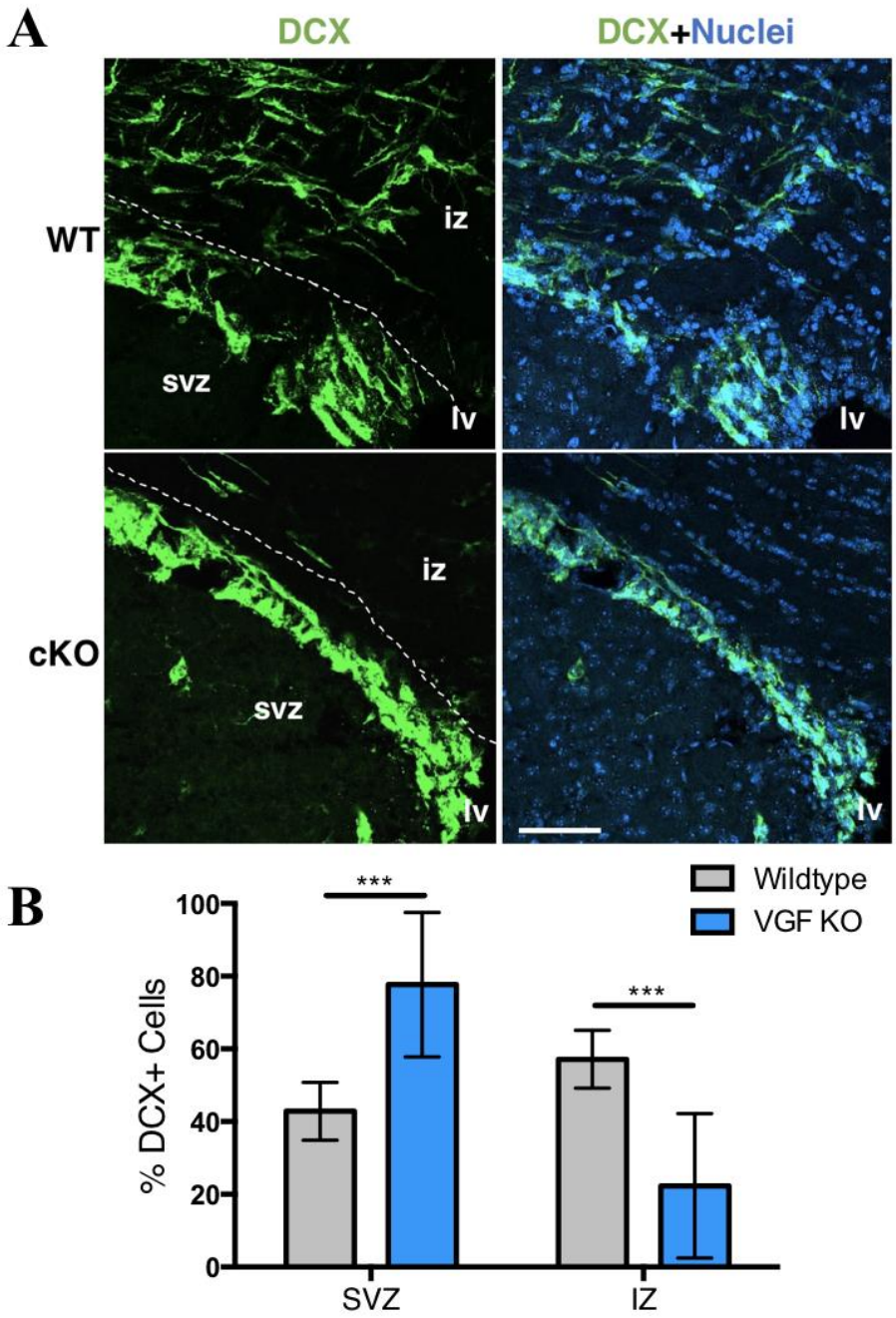

Figure 9. VGF:Nestin-cre knockout mice show reduced migration of neural stem cells post-stroke compared to wildtype littermates. A. Immunofluorescent staining of cortical sections in 8-week-old VGF;Nestin-cre knockout mice and $VGF_{flox/flox}$ littermates (WT) labelled with newborn neuron marker DCX 14-days post-photothrombosis, quantified in B. (n=3 WT, 3 KO), (svz=subventricular zone, lv=lateral ventricle, iz=intermediate zone between lv and infarct). Scale bar = 100μm.

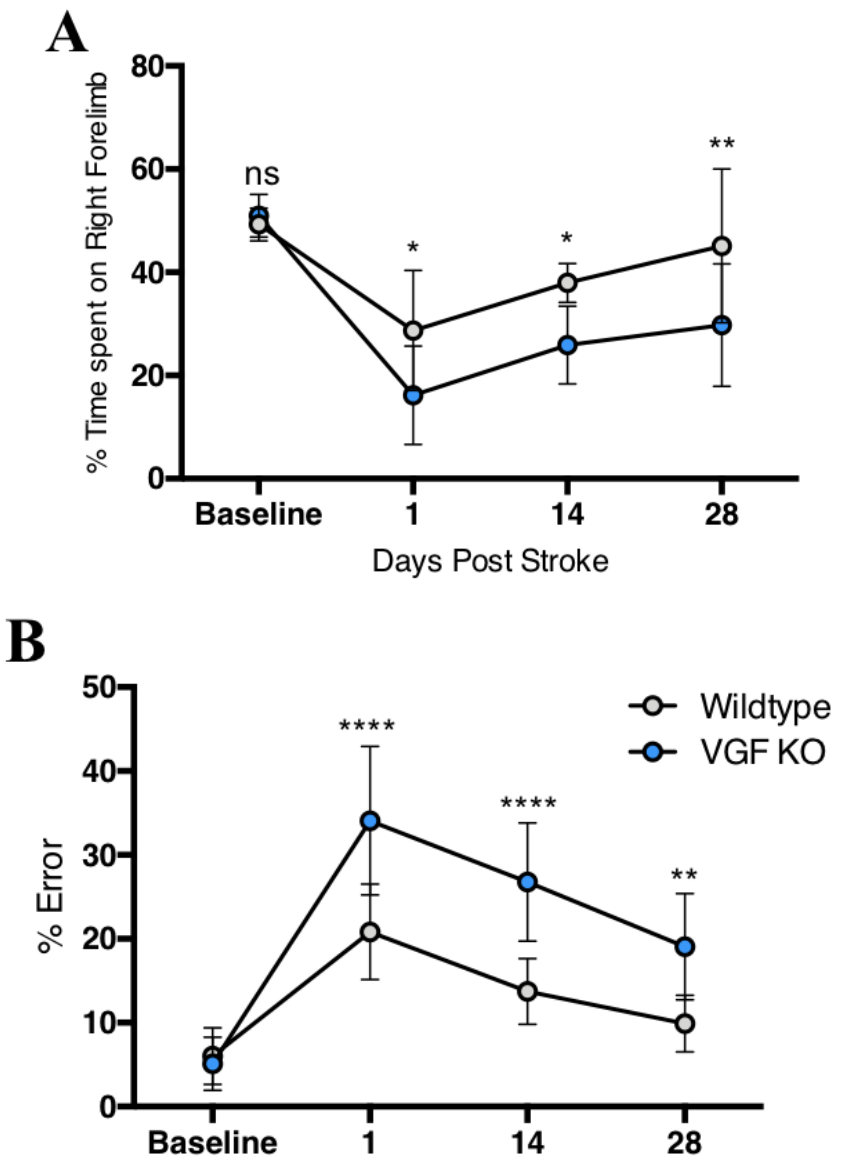

Figure 10. VGF:Nestin-cre knockout mice show significantly larger behavioural deficits post-stroke. A. Quantification of time spent on right forelimb during Cylinder behavioral test pre- and post-photothrombosis (1, 14, 28 days) on 8-week-old VGF;Nestin-cre knockout mice and $VGF_{flox/flox}$ littermates (WT). Significant effect of time ($F(2,34)=10.84$, $p=0002$), interaction ($F(2,34)=0.1487$, $p=0.08624$) and genotype ($F(1,17)=19.30$, $p=0.0004$), (n= 9 WT, 9 KO). B. Quantification of % Error in Horizontal Ladder behavioral test pre- and post-photothrombosis (1, 14, 28 days) on 8-week-old VGF;Nestin-cre knockout mice and $VGF_{flox/flox}$ littermates (WT). Significant effect of time ($F(3,48)=61.40$, $p<0001$), interaction ($F(3,48)=7.902$, $p=0.0002$) and genotype ($F(1,16)=27.41$, $p<0.0001$), (n= 9 WT, 9 KO).

3.2. Overexpression of VGF promotes recovery in post-stroke animals

3.2.1 Increased expression of VGF is present surrounding the lateral ventricles post-AdVGF injection.

We next sought to determine if the reintroduction of exogenous VGF could influence the post-stroke recovery process in mice. As previously mentioned (**section 2.3.2**), an adenoviral vector containing full-length VGF was used in a series of *in vivo* experiments in adult mice post-ischemia. Preliminary investigation to examine the expression pattern of VGF after exogenous delivery has shown that at 14-days post-photothrombosis induced ischemia we observed a noticeable increase in VGF expression compared to mice receiving an AdLacZ control virus injection. Using immunofluorescence, a VGF-specific antibody demonstrated that this increase in expression was mainly concentrated around the lateral ventricles (**Figure 11**).

3.2.2 Upon exogenous delivery of VGF, lateral ventricular areas show increased production and migration of newborn neurons.

An increase in VGF-expression surrounding the lateral ventricles in mice that were administered AdVGF post-ischemia led us to further examine the production of newborn neurons. Using immunofluorescent staining of cortical sections, 14 days post-ischemia, we observed significant differences in the production of DCX+ newborn neurons. We observed a significant increase (~15%) in the quantity of DCX+ cells surrounding the lateral ventricle in *VGF* cKO mice that were administered AdVGF compared to VGF cKO animals with AdLacZ injections (**Figure 12**). Some of the DCX positive newborn neurons in these mice appeared to be migrating away from the lateral ventricle areas, compared to knockout mice that received the control adenovirus.

3.2.3 Intravenous administration of Adenoviral-VGF increases migration of newborn neurons from subventricular zone

As previously mentioned (**section 2.3.2**), an adenoviral vector containing full-length VGF was intravenously administered to *VGF* cKO mice 24 hours post-photothrombosis induced ischemia. After 4-weeks of recovery, cortical sections of the peri-infarct regions from *VGF* cKO mice were labelled with DCX antibodies to identify newborn neurons migrating from the subventricular zone. We observed an increase in migration of newborn neurons towards the peri-infarct region of *VGF* cKO mice that received the VGF-adenovirus when compared to the *VGF* cKO mice that received a control adenovirus (**Figure 13A, B**). We then assessed the behavioural recovery of the VGF cKO mice upon Ad-VGF administration and measured behavioural deficits for one-month post-stroke. Results from the horizontal ladder test showed that cKO mice that received the AdVGF post-stroke reduced their rate of error by 14% (**Figure 14A)**. Concomitantly, the cylinder test concluded that these mice spent significantly more time (10%) on their affected forelimb (**Figure 14B)**.

To further investigate the ability of exogenous VGF to influence the migration of newborn neurons in the peri-infarct region, we also administered the adenovirus to WT mice, post-photothrombosis induced ischemia. Similarly, we observed enhanced migration of newborn neurons in the peri-infarct region using immunofluorescent labelling of DCX, which showed that WT mice that received the VGF-adenovirus saw an increase in the migration of newborn neurons to the damaged region of the brain compared to control WT mice (**Figure 13C, D**).

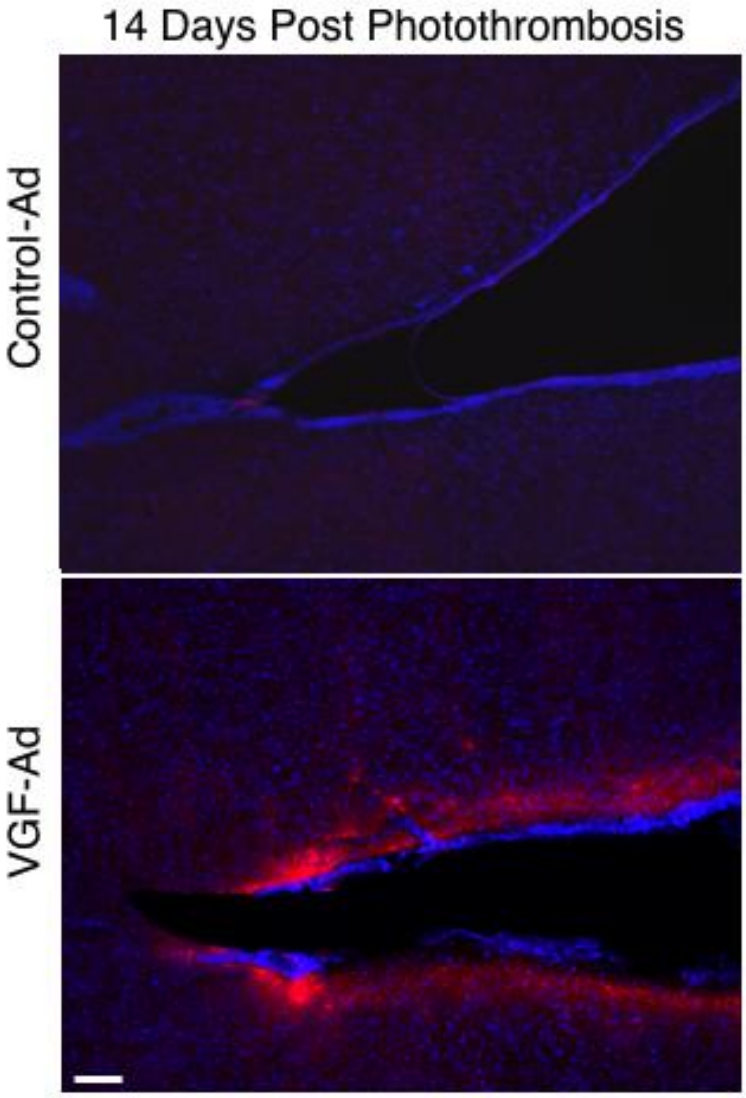

Figure 11. Increased expression of VGF surrounding lateral ventricles in VGF-adenovirus treated mice. Immunofluorescent staining of cortical sections labelled with VGF antibody (red) in 8-week-old C57BL6 (WT) mice, 14 days post-injection of AdVGF or AdLacZ post-photothrombosis. Sections are counterstained with DAPI (blue). Scale bar = 100μm.

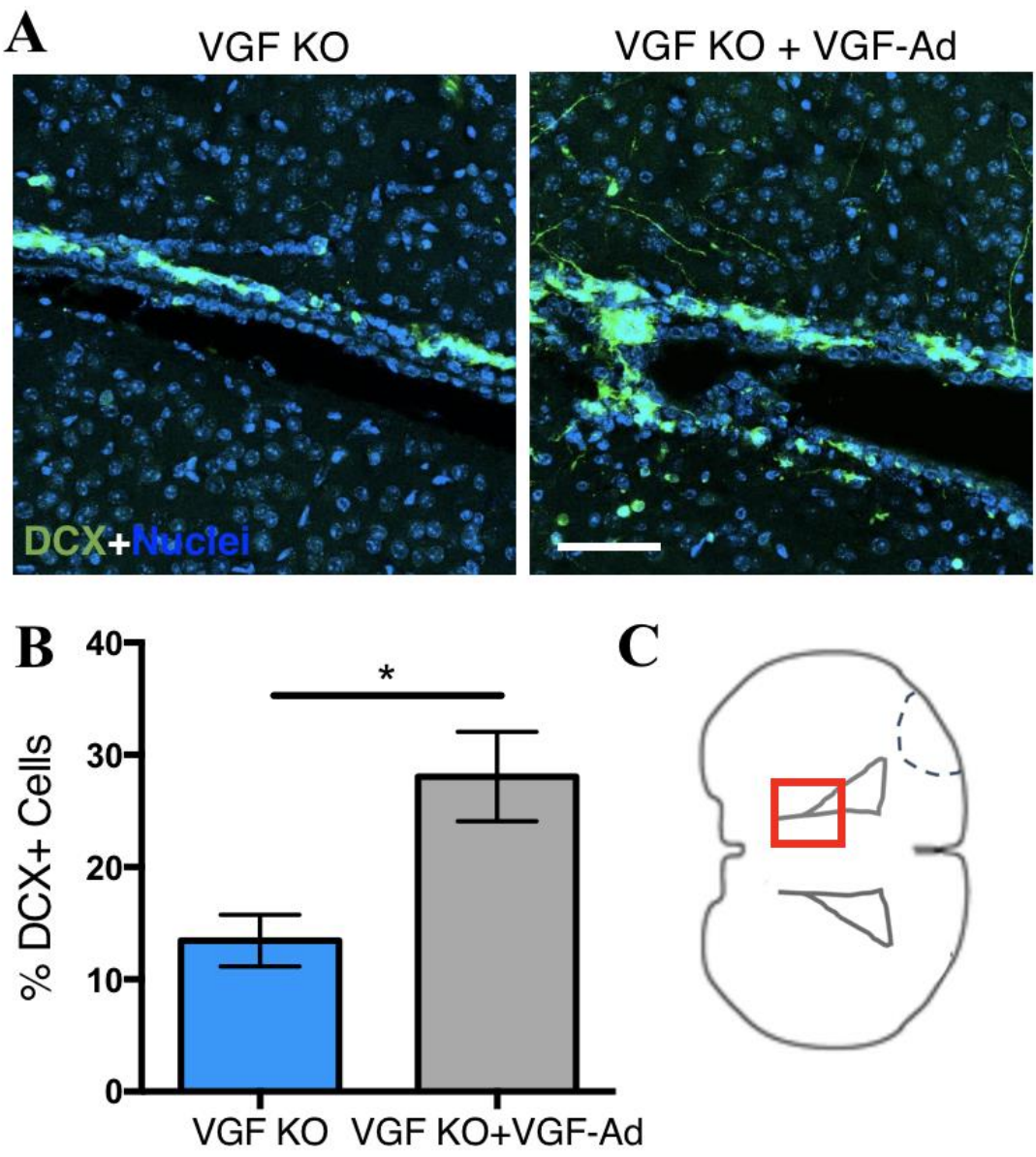

Figure 12. Increased production of newborn neurons surrounding lateral ventricle in *VGF* cKO **mice treated with AdVGF.** A. Immunofluorescent staining of the lateral ventricle of cortical sections from adult mice 14-days post-photothrombosis, labelled with newborn neuron marker DCX (green) and counterstained with DAPI (blue). The number of DCX+ cells are quantified in B. (t=4.503, df=3, p=0.0459), (n=3 VGF KO, 3 VGF KO+VGF-Ad). Scale bar=100μm. C. Coronal section of adult murine brain showing the location (red box) near the subventricular zone (SVZ) of the images in panel A.

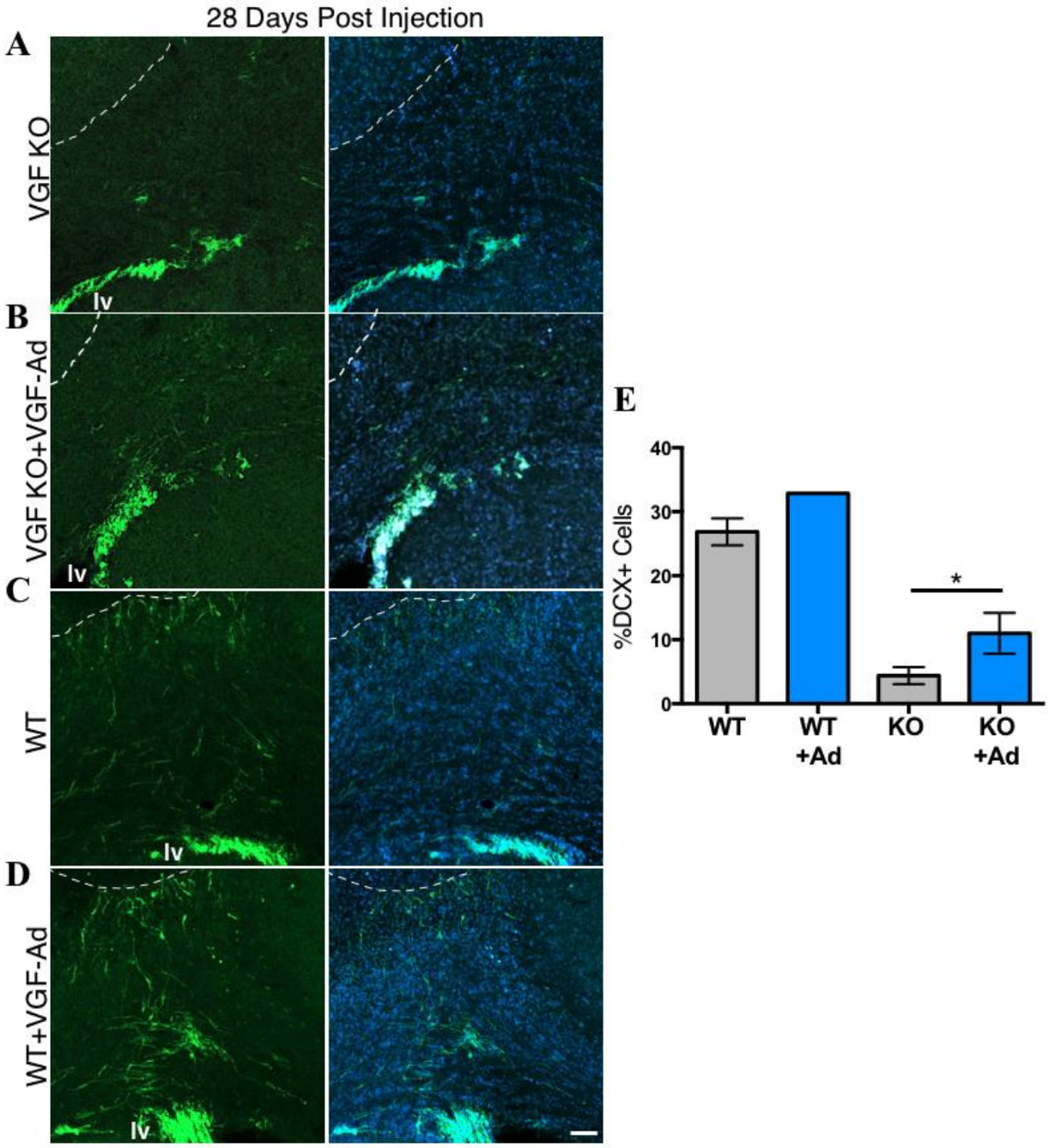

Figure 13. Exogenous delivery of VGF increases migration of neural stem cells in VGF;Nestin-cre knockout mice. A-D. Immunofluorescent staining of cortical sections from adult mice, 28-days post-adenoviral injection, 30 days post-photothrombosis, labelled with newborn neuron marker DCX (green) while cell nuclei are counterstained with DAPI (blue) quantified in E (% if cells labelled with DCX within peri-infarct region) White dotted lines indicates the location of the peri-infarct region. Scale bar = 100μm. lv=lateral ventricle.

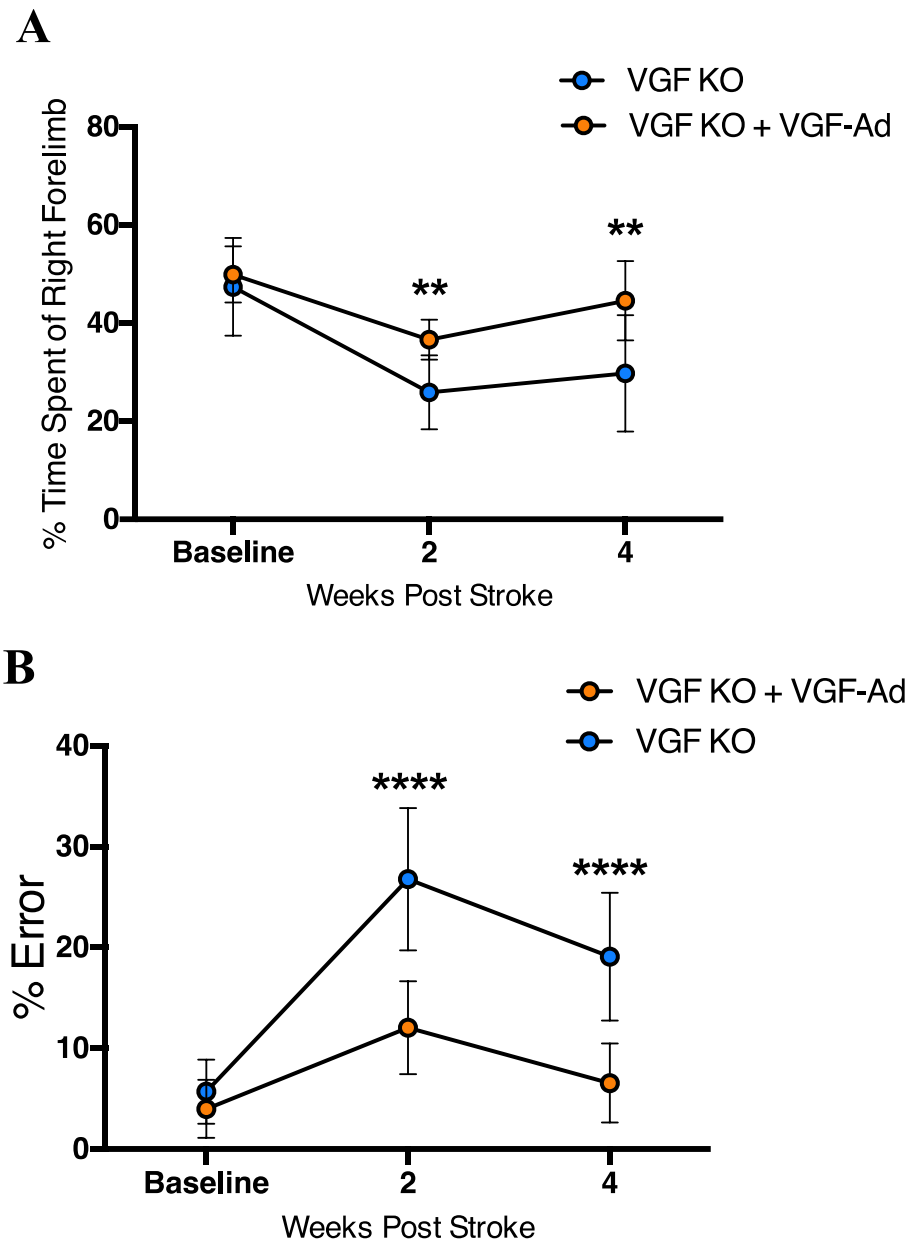

Figure 14. VGF cKO Mice treated with VGF-adenovirus post-stroke show decreased behavioral deficit. A. Quantification of time spent on right forelimb during Cylinder behavioral test pre- and post-photothrombosis and adenoviral injection (2 and 4 weeks) on 8-week-old VGF cKO mice. Adenoviral injection of a VGF-adenovirus or control-adenovirus 2-days post-photothrombosis. Significant effect of time ($F(2,60)=49.54$, $p<0.0001$), interaction ($F(4,60)=1.829$, $p=0.1350$) and genotype ($F(2,30)=10.07$, $p=0.0005$), (n=10 VGF cKO, 9 VGF cKO+AdVGF). Error bars represent standard deviation. Quantification of % Error in Horizontal Ladder behavioral test pre- and post-photothrombosis and adenoviral injection (2 and 4 weeks) on 8-week-old VGF cKO mice. Adenoviral injection of a VGF-adenovirus or control-adenovirus 2-days post-photothrombosis. Significant effect of time ($F(2,58)=67.84$, $p<0.0001$), interaction ($F(4,58)=6.081$, $p=0.0004$) and genotype ($F(2,29)=31$, $p<0.0001$). (n=9 VGF cKO, 9 VGF cKO+AdVGF). Error bars represent standard deviation.

3.2.4 Adenoviral delivery of VGF results in significantly less severe behavioural deficits post-ischemia.

To further investigate the effects of exogenous delivery of VGF using an adenoviral delivery system (AdVGF), we performed several behavioural tests on mice post-photothrombosis induced ischemia to compare behavioural deficits to a control group. Using the horizontal ladder test (**section 2.4.2**), we were able to determine that WT mice who received AdVGF had a significantly lower rate of error compared to WT mice that received a control adenovirus (AdLacZ; **Figure 15A**). Concomitantly, the cylinder test concluded that mice who were given the AdVGF spent more time on their affected forelimb while completing the test (**Figure 15B**). Additionally, horizontal ladder testing was performed at 2 days post-injection to determine the extent of the initial deficit, with no difference between the mice that received AdVGF and AdControl (**Appendix B**). Altogether, these results indicated that WT mice who received AdVGF post-ischemia, performed significantly better in the behavioural tests at both 14- and 28-days post stroke compared to AdLacZ controls, indicative of a less significant behavioural deficit.

3.3. VGF influences inflammatory processes

3.3.1 Exogenous delivery of VGF appears to coincide with increased infiltration of microglia and macrophages in the peri-infarct region.

The post-ischemic inflammatory response is an incredibly influential step in the mediation of both ischemic damage and recovery. The dual role of cellular destruction and pathogen clearance make post-stroke neuroinflammation a delicate part of the recovery process. Our earlier findings indicated that VGF promotes the migration of newborn neurons towards the peri-infarct region, and led us to examine the influence of VGF on the post-stroke inflammatory response. Using

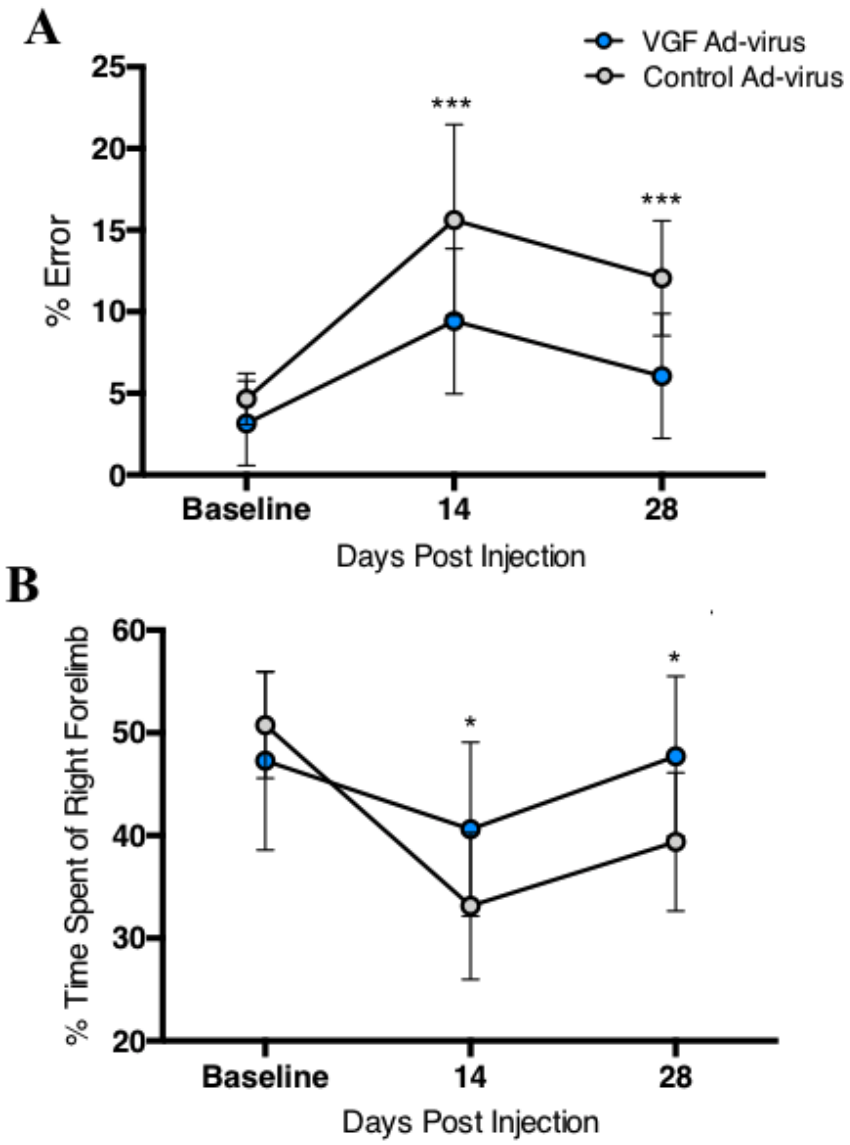

Figure 15. Mice treated with VGF-adenovirus post-stroke show decreased behavioral deficit. E. Quantification of % Error in Horizontal Ladder behavioral test pre- and post-photothrombosis and adenoviral injection (14 and 28 days) on 8-week-old C57BL6 WT mice. Adenoviral injection of a VGF-adenovirus or control-adenovirus 2-days post-photothrombosis. Significant effect of time ($F(2,54)=44.84$, $p<0001$), interaction ($F(2,54)=4.248$, $p=0.0193$) and genotype ($F(1,27)=21.82$, $p<0.0001$), (n=14 Control-Ad, 16 VGF-Ad). F. Quantification of time spent on right forelimb during Cylinder behavioral test pre- and post-photothrombosis and adenoviral injection (14 and 28 days) on 8-week-old C57BL6 WT mice. Adenoviral injection of a VGF-adenovirus or control-adenovirus 2-days post-photothrombosis. Significant effect of time ($F(2,50)=18.34$, $p<0.0001$), interaction ($F(2,50)=5.364$, $p=0.0078$) and genotype ($F(1,25)=6.244$, $p=0.0194$), (n=11 Cont-Ad, 13 VGF-Ad). Error bars represent standard deviation.

WT mice injected with AdVGF or AdLacZ post-photothrombosis, we examined the infiltration of inflammatory cells surrounding the damaged portion of the cortex. Immunofluorescent stained cortical sections were assessed for inflammatory cells using Iba1 antibodies that specifically label microglia and macrophages. At two days post-injection, there was no significant difference in the number of Iba1 cells in the peri-infarct region between the groups. At 14 days post-injection we observed an increase in the quantity of Iba1 positive microglia/macrophages surrounding the infarct in the cortex of both groups, however, there was a statistically significant increase in the number of microglia/macrophages in the AdVGF-treated animals (**Figure 16**).

3.3.2 Absence of VGF doesn't result in significant reduction in post-ischemic inflammatory response

To complement the analysis showing that exogenous VGF increases the inflammatory cell infiltration, we wanted to determine if the absence of VGF results in less microglia/macrophage recruitment to the peri-infarct region of the brain. Using Iba1 immunofluorescence staining of post-photothrombosis cortical sections from adult *VGF* cKO and WT mice, we observed a similar extent of infiltration in both the *VGF* cKO mice and the WT littermates at 14 days post stroke, suggesting that they have similar levels of post-stroke inflammation (**Figure 17**).

3.3.3 VGF peptide TLQP-21 is most efficient at promoting the migration of Raw267.4 macrophages

VGF is processed into many secreted peptides that are responsible for a wide variety of biological processes. To further investigate the effects of VGF on inflammation, we tested several of the most well characterized VGF-derived peptides. C-terminal peptides TLQP-21, TLQP-62 and LQEQ-19 were used to treat Raw267.4 cells in a migration assay. Migration was

assessed using a chamber style method in which cells could migrate through a membrane towards a second chamber containing varying concentrations of peptides, thereby determining the chemotaxis properties of individual peptides. It was apparent that both the TLQP-based peptides were the most effective at attracting the macrophages as we saw over 126 and 529 cells migrating through the membrane per FOV when using TLQP-62 and TLQP-21 respectively, compared to just 13 using LQEQ-19 (**Figure 18**). Optimization of TLQP-21 concentration increased the number of migrated cells from 262 cells (1nM) to 529 (10nM), a two-fold increase (**Figure 18**).

3.3.4 TLQP-21 peptide influences cell migration via the C3a receptor

As we had previously observed, VGF-derived TLQP-21 proved to be the most effective peptide at influencing the migratory activity of macrophages. To further delineate the mechanism behind these effects, we investigated two well-known receptors of TLQP-21 to determine which one the TLQP-21 peptide was signalling through to stimulate migratory activity. As mentioned (**section 1.2.4**), TLQP-21 has been shown to signal through complement receptors C3aR and gC1qR and function in a wide variety of biological roles. Using inhibitors for both receptors, we repeated the migration assay using Raw264.7 cells treated with TLQP-21 peptide (**Figure 19**). We observed that inhibition of C3a or the gC1q receptors reduced the number of cells that migrated through the membrane, while their effectiveness differed greatly. The migratory activity of Raw 264.7 cells treated with TLQP-21 was reduced by 90% when inhibiting the C3a receptor compared to a reduction of only 20% upon gC1qR inhibition, whereas using a C3a agonist showed a similar number of migrated cells to the treatment with TLQP-21.

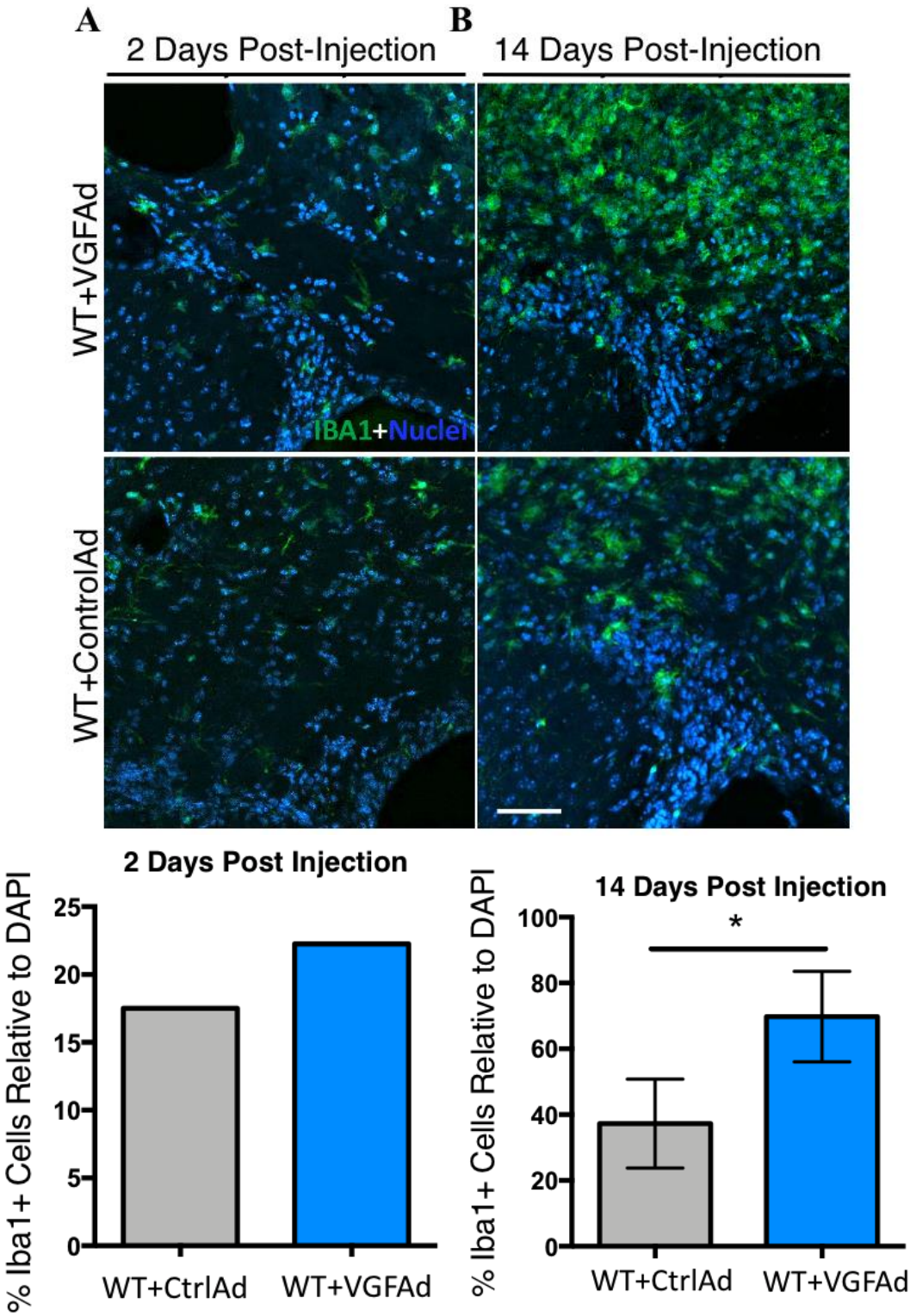

Figure 16. Increased infiltration of inflammatory cells in peri-infarct region 14 days post injection of AdVGF. Immunofluorescent staining of the peri-infarct region of cortical sections from WT adult mice 2 and 14-days post-injection, labelled with microglia/macrophage marker Iba1, Quantigied in C and D ($p = 0.043$). Scale bar=100μm.

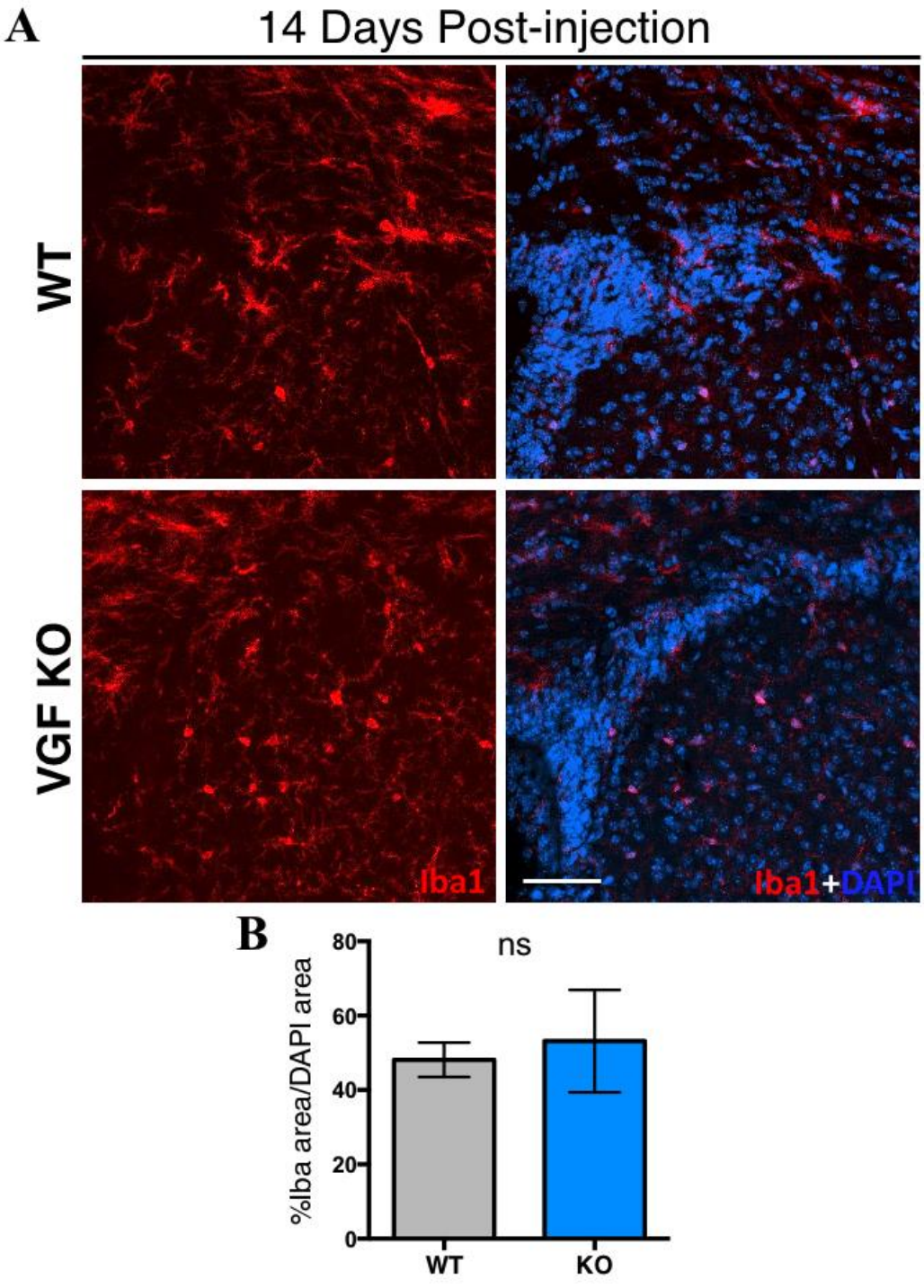

Figure 17. No significant change in inflammatory response post-ischemia in VGF:Nestin-cre knockout mice. A. Immunofluorescent staining of the peri-infarct region of cortical sections from adult mice 14-days post-stroke, labelled with microglia/macrophage marker Iba1 quantified in B. (WT: n=3, KO: n=3). Scale bar=100μm.

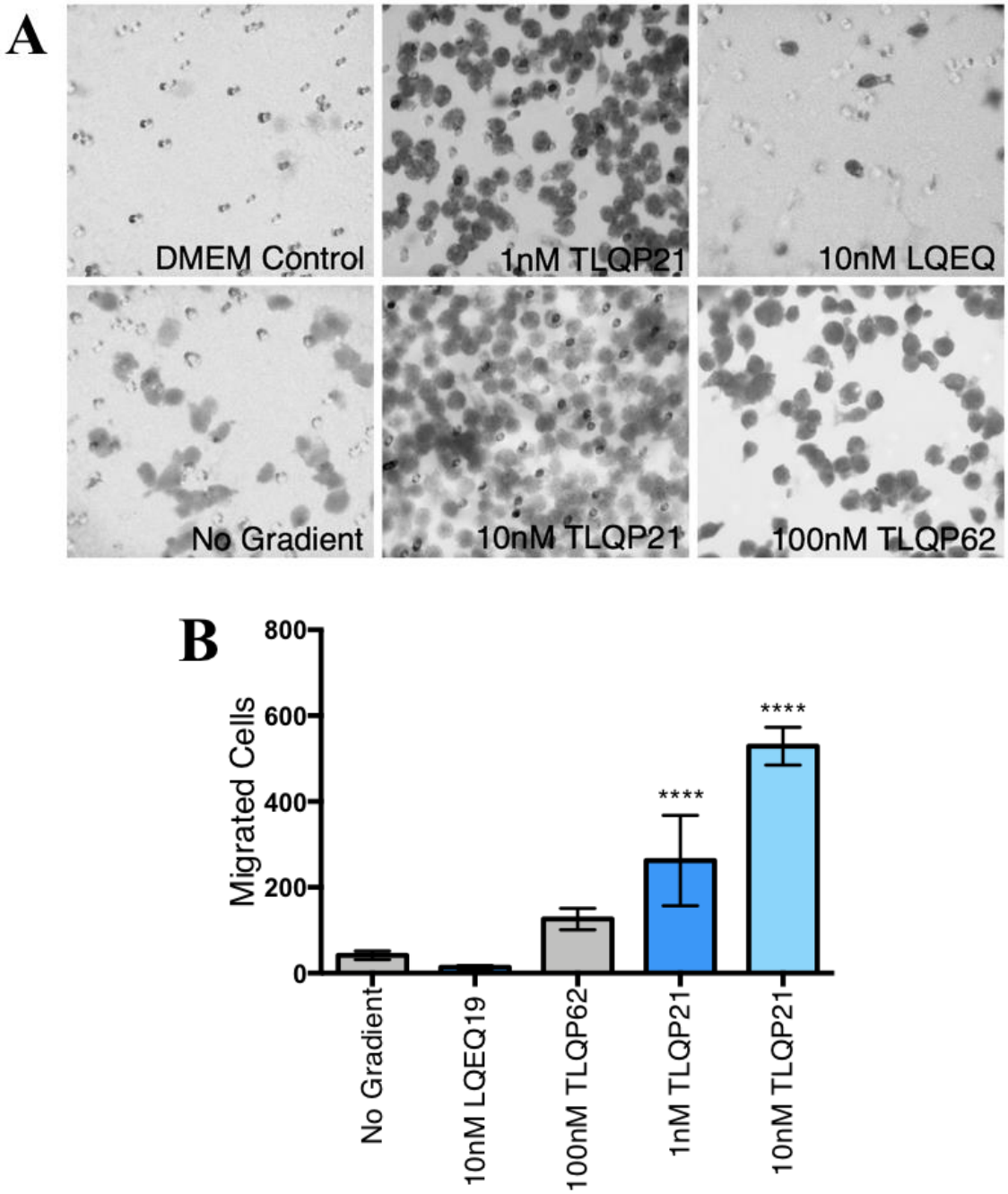

Figure 18. C-terminal peptide TLQP-21 influences migration of Raw264.7 macrophages. A. Migration assay using RAW264.7 cells demonstrated chemoattractant properties of VGF C-terminal peptides, quantified in B. B. Significant results were seen in groups treated with 1nM TLQP21 ($p=0.0144$) and 10nM TLQP21 ($p<0.001$) when compared to control group (no gradient).

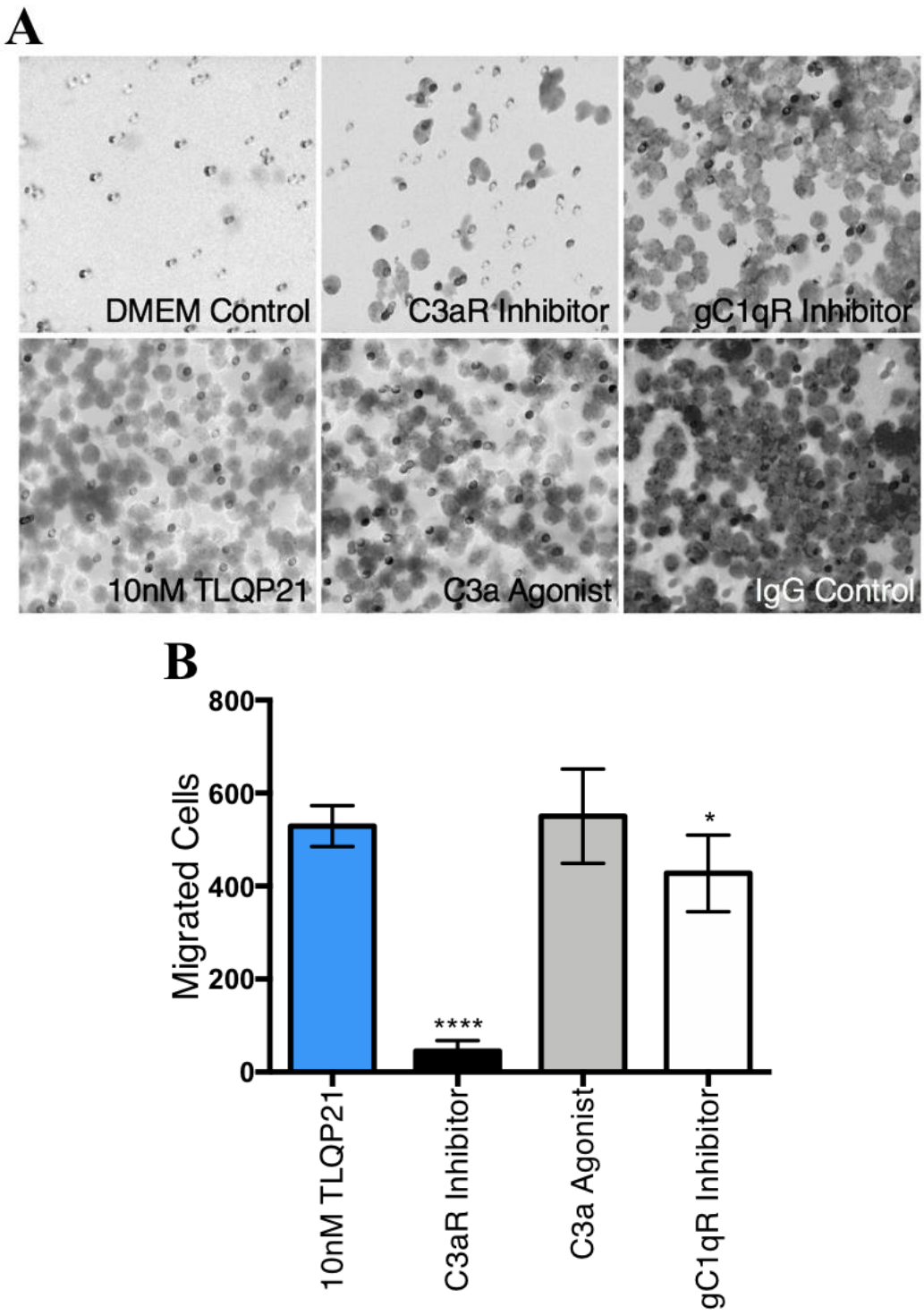

Figure 19. C-terminal VGF peptide TLQP-21 signals primarily through C3a receptor. Migration assay using inhibitors and agonists of known TLQP-21 receptors using RAW264.7 cells treated with 10nM TLQP21 quantified in D. D. Significant results were seen in the C3aR inhibitor treatment group ($p<0.0001$)

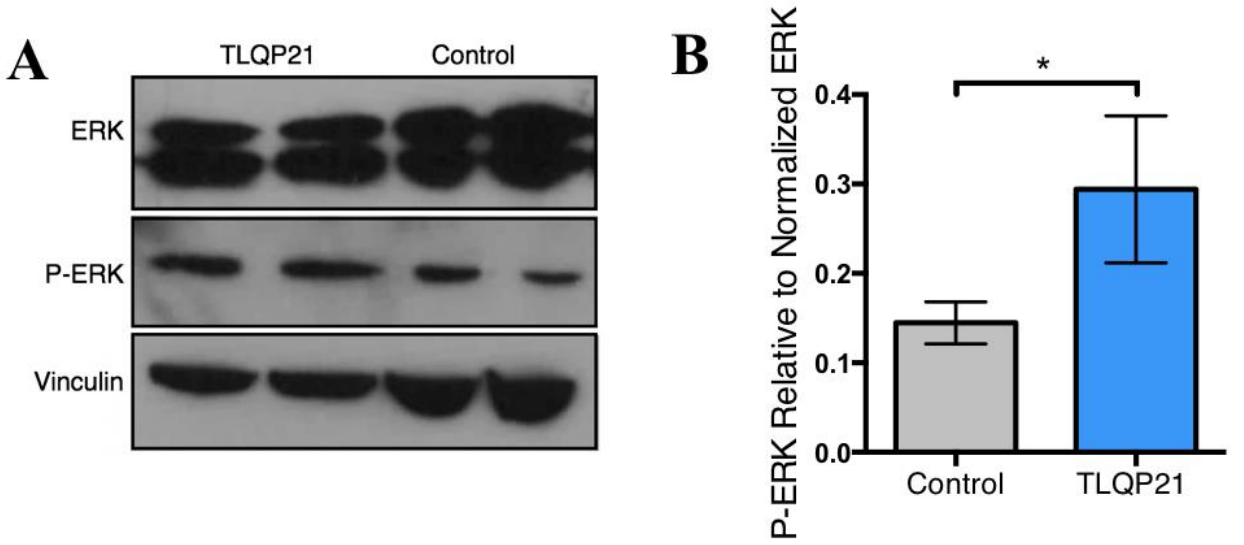

Figure 20. TLQP-21 activates cell survival pathways in TLQP-21 macrophages. A. Immunoblot of RAW264.7 cells treated with TLQP21 or control (DMEM) indicating phosphorylation of resident ERK population quantified in B. (t=3.492, df=6, p=0.0129), (n=4 TLQP-21, 4 WT). Error bars represent standard deviation.

3.3.5 Increased activation of cell survival pathway upon treatment with TLQP21 in Raw267.4 macrophages

C3aR signalling is known to activate through the ERK1/2 pathway to mediate cell proliferation, migration, inflammation and cell survival[124]. As such, we used immunoblot assays to assess changes in the phosphorylation of ERK, indicative of increased or decreased activation. First, we determined the normalized ERK and P-ERK population relative to a control protein (vinculin), which allowed us to calculate the percentage of resident ERK that is phosphorylated (**Appendix C**). Compared to untreated cells, the TLQP-21 treated cells showed a significant increase in phosphorylation of the resident ERK population, indicative of activation (**Figure 20**).

4. Discussion

VGF has long been associated with the pathology and etiology of neurological diseases such as stroke, however, very little has been done to investigate the detailed mechanisms behind its function. These preliminary findings are the first to define the roles of VGF in ischemic pathology and its influence on post-ischemic functional recovery and the migration of newborn neurons and inflammatory cells.

4.1 VGF is necessary for 'typical' post-stroke recovery

When an ischemic event occurs, the lack of oxygenated blood initiates a cascade of biological processes that have reparative and/or damaging motives. The catastrophic neurological event causes a dysregulation in oxidative phosphorylation which ultimately results in a reduction of ATP, contributing to cellular death and inflammation. This hypoxia-induced cell death triggers the production of downstream cytokines and growth factors that participate in endogenous repair mechanisms such as EPO, VEGF, IGF-1 and BDNF[125]. Although necessary for normal functioning of the central nervous system, these factors activate multiple signalling pathways in the microenvironment of the peri-infarct region that are involved in the mediation of apoptosis, revascularization, inflammation, cell differentiation and proliferation post-ischemia[125].

Consistent with previous evidence from Sakamoto *et al.*[112], VGF and BDNF are significantly upregulated in peri-infarct cortical tissue of WT mice 2 days post-ischemia (**Appendix B**). This is consistent with other findings that indicate a positive feedback loop of VGF-BDNF in the brain is essential for hippocampal function and synaptic transmission[23]. The significant increase of VGF post-ischemia suggests its importance in the post-stroke recovery

processes, similar to its autoregulatory partner BDNF. It is difficult to determine whether the increase in VGF expression post-ischemia results in an increase in growth factors such as BDNF, or vice versa.

Upon removal of VGF in a transgenic cKO mouse model, there are no significant developmental or behavioural abnormalities compared to WT littermates. Although they display a significant reduction in body fat, the size of their brain is unchanged (**Figure 4**). The cortical development of these mice appears normal compared to their WT littermates with no significant changes in cortical layer markers (**Figure 5**). The baseline motor function of VGF cKO mice is also normal, suggesting that the removal of VGF doesn't have any significant motor function impairments, allowing for an accurate comparison of post-stroke behavioural deficits (**Figure 6**).

Photothrombotic induced ischemia in the left sensorimotor cortex in VGF cKO and WT mice resulted in significant functional impairments lasting at least 28-days post-ischemia (**Figure 10**). Behavioural analysis measuring motor function and forelimb asymmetry has shown that VGF cKO mice have a significant improvement in behavioural recovery compared to WT mice (**Figure 10**). This discrepancy in motor function is present from the initial behavioural testing timepoint, 2 days post-ischemia, suggesting that the absence of VGF augments post-stroke behavioural deficits. Magnetic resonance imaging of the infarcted region in both VGF cKO mice and WT littermates 24 hours post-stroke show similar infarct regions of approximately $8mm^3$ (**Figure 8**). The absence of any changes in infarct volume between the VGF cKO and WT mice indicate that the behavioural deficit observed wasn't due to the portion of the brain that was damaged, suggesting that a change in the post-stroke repair processes is responsible.

Upon ischemic stroke, a large number of newborn neurons are generated in the subventricular zone of the cortical region and have been shown to migrate towards the damaged region of the brain[126]. It has been hypothesized that only a small number of these cells are able to integrate into the neural network and function properly, while others could provide trophic support to facilitate repair processes[97,127]. Further investigation into these newborn neurons generated through neurogenesis in the subventricular zone of VGF cKO mice showed significant differences in their migration toward the infarct (Figure 9). Typically, there is a portion of newborn neurons originating from the lateral ventricle that migrate towards the damaged region of the brain, proposed to participate in brain recovery processes. The DCX+ newborn neurons in the VGF cKO mice were sequestered to the lining of the lateral ventricle while WT mice showed nearly 40% more neurons migrating towards the damaged region of the brain (**Figure 9**).

Through the absence of VGF in adult mice, the post-ischemic response is significantly disrupted on both the functional and cellular levels. The notable difference in post-stroke behavioural deficits in VGF cKO mice continues throughout the 28 days of behavioural testing (Figure 10), while still maintaining a steady improvement in their recovery. The histological findings of significantly reduced migration of newborn neurons suggests that VGF may play a role in the migration of these cells towards the damaged portion of the brain. The overall effects caused by VGF deletion and the subsequent disruption of growth factor levels in the peri-infarct microenvironment (such as BDNF), seem to significantly impair the ability of these mice to recover similarly to their WT littermates. Inhibiting the normal migration of neurons as well as causing larger motor deficits, highlights the ability of VGF to influence the post-stroke recovery phase, as well as it's necessity for normal post-stroke recovery.

4.2 Exogenous delivery of VGF improves post-stroke behavioural recovery and influences migration of newborn neurons in peri-infarct region.

While the present study was able to determine that the absence of VGF seems to contribute to more significant behavioural deficits and reduced migration of newborn neurons, we sought to also examine the effects of reintroducing VGF during the post-stroke recovery phase. During this phase, the brain is in a state of shock creating a microenvironment surrounding the damaged region of the brain where high concentrations of growth factors and cytokines are present[128]. A modification or disruption of these factors has been shown to influence the normal processes that prevent secondary brain damage post-stroke and aid in brain repair[128,129]. Prior to this study, adenoviral delivery of VGF *in vivo* was used to improve neurodevelopmental deficits, specifically in the cerebellum, and ameliorate early post-natal lethality in Snf2h cKO mice.

Utilizing adenoviral delivery of VGF, we used intravenous administration of adenoviral VGF in WT mice and found an increase in histological expression of VGF surrounding the lateral ventricles, confirming that there was a change in VGF expression (**Figure 11**, **Appendix A**). It was noted that the full-length VGF protein is relatively large and may not have the ability to cross the blood-brain barrier, but the proteolytic cleavage of VGF into a wide range of peptides allows it to function as a group of tiny peptides (predominantly C-terminal), which could explain the change in expression. The activity-dependant properties of VGF also could explain the change in VGF expression seen upon exogenous delivery, which could elicit a systemic response which in turn increases VGF throughout the neuroendocrine system.

Once we tested the adenoviral delivery of VGF, we introduced it into VGF cKO mice 2 days post-photothrombosis. This resulted in an 8% reduction in behavioural deficit at multiple timepoints post-stroke, compared to VGF cKO mice that received the control adenovirus (**Figure**

14). In an attempt to further investigate the mechanisms behind this improvement in motor function, we then choose to investigate the endogenous mediators of post-stroke recovery in the peri-infarct region. Looking closely at the migratory activity of DCX+ newborn neurons upon exogenous delivery of VGF, it was clear that there was an increase in the number of cells that were migrating from the subventricular zone to the infarct region compared to VGF cKO mice that received a control adenovirus (**Figure 13**). Additionally, there was an increase in the number of cells migrating from bottom of the lateral ventricle as well, consistent with our previous findings that showed an increase in VGF expression post-exogenous delivery (**Figure 12**). Comparatively, the VGF cKO mice that received AdVGF demonstrated a clear rescue, with 84% of cells migrating towards the peri-infarct region when compared to WT mice while their behavioural deficits were relatively similar throughout their recovery time (**Figure 13**).

The potential for exogenous delivery of VGF to compensate for its absence in the VGF cKO mouse model, begged the question of whether VGF was capable of influencing post-stroke recovery in WT mice as well. The modified processes that we assessed, demonstrated that VGF has the ability to influence migration of endogenous mediators of post-stroke recovery such as newborn neuron migration and a reduction in post-stroke behavioural deficit. Additionally, exogenous delivery of VGF also elicited a modified post-stroke response, specifically regarding the migratory activity of newborn neurons. Similar to the AdVGF-treated VGF cKO mice, there was a large influx of DCX+ newborn neurons that migrated from the subventricular zone of WT mice treated with Ad-VGF towards the damaged portion of the brain (**Figure 13**). Complementary to these results, the behavioural analysis at multiple timepoints post stroke suggested that the mice receiving exogenous VGF performed significantly better and had less of a motor function deficit compared to WT mice that received a control virus (**Figure 15**).

Our study has shown that altered levels of VGF in the brain microenvironment, whether endogenous or exogenous, results in significant changes in post-stroke recovery. The neuronal microenvironment facilitates the post-stroke repair processes such as the proliferation and differentiation of neuroprogenitors post-ischemia[128]. Previous studies have demonstrated that this increase in neuronal migration towards damaged regions of the brain is often paralleled with improved behavioural recovery[130,131]. However, it has also been shown that very few newborn neurons that migrate towards the infarct region are capable of integrating into the neural circuitry, begging the question of how altering the migration of newborn neurons affects behavioural recovery and the associated mechanisms[97].

Due to its autoregulatory properties, changes in the expression of VGF specifically in the cortical region ultimately modifies the levels of BDNF and possibly other factors and cytokines that facilitate brain repair mechanisms such as synaptogenesis and revascularization. Areas around the lateral ventricle that were highly saturated with VGF expression, appear to promote the proliferation and migration of neuroprogenitors, which have the ability to activate signalling pathways and secrete a number of factors, all contributing to an overall repair-positive microenvironment at the peri-infarct region[132,133]. By increasing the overall number of migrating neurons in the peri-infarct region as well as the pace at which they migrate, the post-stroke effects of altered VGF expression may enhance the reparative environment and promote functional recovery through the secretion of trophic factors and facilitation of repair processes.

4.3 VGF secreted peptides influence inflammatory cell migration *in vivo* and *in vitro*

Ischemia and oxygen deprivation trigger a cascade of neurological events within the peri-infarct region including inflammatory responses, oxidative stress and ultimately apoptosis[134]. The

inflammatory response plays a significant role in the post-stroke recovery phase and is managed by the resident macrophage population of microglia. These cells are responsible for monitoring the neural environment for changes and triggering both detrimental and neuroprotective effects in response[134]. VGF receptor C3aR has been shown to be a key mediator of these detrimental and neuroprotective processes through its downstream pathways influencing phagocytosis and pathogen clearance[64,135]. Using a Snf2h dKO mouse model where C3aR was also deleted, a significant increase in behavioural deficits was observed compared to the Snf2H cKO mice, specifically due to a reduction in debris clearance and enhanced gliosis[64]. The ability of C3aR to mediate these responses has also been tested using C3a-ligand based post-stroke therapeutics that demonstrated a dual role of damage and repair based of the timing of its administration post-stroke[40,136]. The conflicting nature of complement protein C3a and its inability to consistently influence positive mediators of post-stroke repair has shifted the focus to other therapeutic targets that signal through the C3a receptor, such as VGF-derived peptide TLQP-21.

Our study has demonstrated that altered levels of VGF expression affects endogenous mediators of stroke such as neuroprogenitor cell production and their migration towards the damaged region of the brain. This prompted the investigation of VGF and its effect on the post-stroke inflammatory response, more specifically its effects on inflammatory cells such as microglia and macrophages that often play a key role in the clearance of debris from damaged regions of the brain[137].

The exogenous delivery of VGF to WT mice several days post-ischemia led to a significant influx of Iba1+ microglia and macrophages in the peri-infarct region after 2-weeks of recovery (**Figure 16**). The WT mice also showed a large immune response, which is to be expected after ischemic brain damage. The dual role of inflammatory cells in mediating

damaging and reparative effects makes it difficult to determine if the cells in the peri-infarct region are exacerbating the injury or participating in pathogen clearance and phagocytosis, clearing the damaged region of debris making it easier for the brain to begin repairing and reorganizing it's neural connections and re-establishing blood flow. This significant influx of inflammatory cells to the peri-infarct region coupled with the reduced behavioural deficits seen in mice that received the VGF adenovirus (**Figure 15**), suggests that these inflammatory cells have a predominantly reparative effect on post-stroke recovery. Further investigation into the phenotypic properties of the microglia proved to be a challenge due to the large influx of Iba1+ cells in the infarct region, making it difficult to discern morphology of these cells.

Knowing that VGF has the capability to modify the migration of newborn neurons post-ischemia, while also being able to influence the population of inflammatory cells in the peri-infarct environment, it became clear that VGF played an important role in migration. We investigated the mechanisms behind the changes in migratory activity seen in inflammatory cell populations, as this study is the first of its kind to suggest that VGF plays a role in the migration of endogenous mediators of stroke recovery. VGF itself does not typically function as one neuropeptide, but rather, a large number of neuropeptide fragments signalling through a wide variety of pathways. It was crucial to determine if this chemotactic effect was attributed to a single VGF peptide and through which pathway it functioned. The small C-terminal peptide TLQP-21 was the most effective peptide at recruiting inflammatory cells and showed significant chemotactic properties (**Figure 18**). As previously mentioned, TLQP-21 is one of the more well characterized VGF peptides with two proposed receptors, C3aR and gC1qR (**section 1.2.4**). Our *in vitro* findings have shown that through the deactivation of the C3a receptor, C3aR, the chemotactic influence of TLQP-21 on inflammatory cells was substantially diminished (**Figure**

19). Through the inhibition of this receptor, we were able to determine that TLQP-21 has the ability to attract inflammatory cells by signalling through the C3aR receptor. This study is the first to propose that a specific VGF-derived peptide is responsible for influencing the migration of inflammatory cells through the C3a receptor rather than the alternative gC1q receptor. The C3a receptor is present on the surface of both inflammatory cells (microglia/macrophages) as well as neural stem cells and neural progenitors, making it plausible that this signalling pathway could be responsible for the migratory effects previously shown[138].

Similar to other G-protein coupled receptors, the C3a receptor activates many downstream signalling pathways involved in a wider variety of biological processes. One of these pathways, the extracellular signal-regulated kinase (ERK/MAPK pathway), has a long history of being involved in the morphology and migration of various cell types[139]. Previous findings using a pharmacologic activator of the ERK/MAPK pathway have demonstrated that upon activation, there is an increase in expression of cell survival genes (c-Fos, c-Jun) as well as protective detoxifying enzymes resulting in survival and protective mechanisms[140]. Activation of the ERK pathway has also been indicated as one of the critical regulators of cell motility along with cell proliferation and differentiation, making it a good candidate for further investigation[140]. We discovered, that the resident ERK population in inflammatory cells treated with TLQP-21 showed a significant increase in phosphorylation compared to untreated cells (**Figure 20**). This increase in phosphorylation is indicative of activation of this pathway and its downstream targets, such as pro-survival mechanisms and suppression of apoptosis[141]. This newly proposed mechanism for TLQP-21 signalling via C3aR resulting in an activation of the ERK signalling pathway and ultimately affecting cellular motility and survival, could explain the migratory phenotypes observed in this study. However, further investigation into the exact downstream

mechanisms of the ERK pathway and its influence on reparative vs. destructive inflammatory activation is necessary.

5.4 Future directions

This study is the first to define the role of VGF and its derived peptides in the migration of endogenous mediators of stroke recovery. However, while we have suggested that the influence of VGF on the migration of newborn neurons and inflammatory cells affects the peri-infarct microenvironment, further investigation into the participation of these cell types in post-stroke recovery is necessary. We are still uncertain as to what role newly generated neurons play in the post-ischemic brain and their influence on post-stroke functional recovery. In models of endogenous overexpression of VGF, we see a significant increase in the number of cells that migrate towards the damaged region, but the effect that these cells have is still undetermined. As previously mentioned, findings from Kannagara *et al* have proposed that the majority of the migrated neurons in the peri-infarct region have a very limited capacity to integrate into the cortical network, thus limiting their ability to potentially participate in stroke recovery[97]. Thus, It is crucial that we determine to what extent these cells are able to reintegrate into the neural network and facilitate brain repair processes and reorganization, or if these cells mainly function as more of a supporting role through the secretion of trophic factors and cytokines, creating a repair-positive microenvironment.

We have shown that VGF plays a role in the post-stroke recovery phase and has the ability to attract inflammatory cells and influence their motility. However, it would be interesting to determine the exact effects of these cells and if VGF has the ability to modify the activity, whether it be reparative or destructive, and to what extent. Co-labelling of M1 and M2 microglia

markers in the peri-infarct region of Ad-VGF treated mice could help identify the predominant microglial phenotype and their function (e.g. phagocytosis). Taking a closer look at the role of TLQP-21 receptor C3aR in stroke, would also provide greater insight into the role that VGF plays in the post-stroke inflammatory response. Removing this receptor using a C3aR knockout mouse model treated with Ad-VGF and monitoring their behavioural recovery could indicate whether this pathway is the sole mechanism for VGF and its ability to alter the motility of inflammatory cells. It would be interesting to determine whether these mice would have more significant behavioural deficits than VGF cKO mice treated with ad-VGF, or if there is some sort of compensatory mechanism that can facilitate VGF's post-stroke inflammatory response.

This study has shown the effects of altered VGF expression, both endogenous and exogenous, on functional recovery post-ischemia. The ability of VGF to reduce motor deficits post-stroke was apparent, however further investigation into the connection between the histological findings of increased newborn neuron migration and an influx of inflammatory cells and the improved functional recovery is necessary. While it is clear that VGF and its secreted peptides play a wide variety of roles in neurological conditions such as stroke, the investigation into exact mechanisms and therapeutic capabilities of VGF is in its infancy.

References

1. Burbach JP. What are neuropeptides?. Methods Mol Biol. 2011;789:1-36.
2. Mains RE, Eipper BA. The Neuropeptides. In: Siegel GJ, Agranoff BW, Albers RW, et al., editors. Basic Neurochemistry: Molecular, Cellular and Medical Aspects. 6th edition. Philadelphia: Lippincott-Raven; 1999.
3. Zandawala M, Marley R, Davies SA, Nässel DR. Characterization of a set of abdominal neuroendocrine cells that regulate stress physiology using colocalized diuretic peptides in Drosophila. Cell Mol Life Sci. 2018;75(6):1099-1115.
4. Levi A., Canu N., Trani E., Benedetti M., Possenti R. (1991) VGF: A Tissue Specific Protein and a Marker of NGF-Induced Neuronal Differentiation. In: Bagnoli P., Hodos W. (eds) The Changing Visual System. NATO ASI Series (Series A: Life Sciences), vol 222. Springer, Boston, MA
5. Canu N, Possenti R, Ricco AS, Rocchi M, Levi A. Cloning, structural organization analysis, and chromosomal assignment of the human gene for the neurosecretory protein VGF. Genomics. 1997;45(2):443-6.
6. Salton SR, Ferri GL, Hahm S, et al. VGF: a novel role for this neuronal and neuroendocrine polypeptide in the regulation of energy balance. Front Neuroendocrinol. 2000;21(3):199-219.
7. Lewis JE, Brameld JM, Jethwa PH. Neuroendocrine Role for VGF. Front Endocrinol (Lausanne). 2015;6:3.
8. D'arcangelo G, Habas R, Wang S, Halegoua S, Salton SR. Activation of codependent transcription factors is required for transcriptional induction of the vgf gene by nerve growth factor and Ras. Mol Cell Biol. 1996;16(9):4621-31.
9. Liu PZ, Nusslock R. Exercise-Mediated Neurogenesis in the Hippocampus via BDNF. Front Neurosci. 2018;12:52.
10. Jiang C, Lin WJ, Salton SR. Role of a VGF/BDNF/TrkB Autoregulatory Feedback Loop in Rapid-Acting Antidepressant Efficacy. J Mol Neurosci. 2019;68(3):504-509.
11. Hunsberger JG, Newton SS, Bennett AH, et al. Antidepressant actions of the exercise-regulated gene VGF. Nat Med. 2007;13(12):1476-82.
12. Alvarez-saavedra M, De repentigny Y, Yang D, et al. Voluntary Running Triggers VGF-Mediated Oligodendrogenesis to Prolong the Lifespan of Snf2h-Null Ataxic Mice. Cell Rep. 2016;17(3):862-875.
13. Trani E, Giorgi A, Canu N, et al. Isolation and characterization of VGF peptides in rat brain. Role of PC1/3 and PC2 in the maturation of VGF precursor. J Neurochem. 2002;81(3):565-74.
14. Lin WJ, Jiang C, Sadahiro M, et al. VGF and Its C-Terminal Peptide TLQP-62 Regulate Memory Formation in Hippocampus via a BDNF-TrkB-Dependent Mechanism. J Neurosci. 2015;35(28):10343-56.
15. Severini C, Ciotti MT, Biondini L, et al. TLQP-21, a neuroendocrine VGF-derived peptide, prevents cerebellar granule cells death induced by serum and potassium deprivation. J Neurochem. 2008;104(2):534-44.
16. Toshinai K, Nakazato M. Neuroendocrine regulatory peptide-1 and -2: novel bioactive peptides processed from VGF. Cell Mol Life Sci. 2009;66(11-12):1939-45.

17. Hannedouche S, Beck V, Leighton-davies J, et al. Identification of the C3a receptor (C3AR1) as the target of the VGF-derived peptide TLQP-21 in rodent cells. J Biol Chem. 2013;288(38):27434-43.
18. Cero C, Vostrikov VV, Verardi R, et al. The TLQP-21 peptide activates the G-protein-coupled receptor C3aR1 via a folding-upon-binding mechanism. Structure. 2014;22(12):1744-1753.
19. Possenti R, Muccioli G, Petrocchi P, et al. Characterization of a novel peripheral pro-lipolytic mechanism in mice: role of VGF-derived peptide TLQP-21. Biochem J. 2012;441(1):511-22.
20. Cassina V, Torsello A, Tempestini A, et al. Biophysical characterization of a binding site for TLQP-21, a naturally occurring peptide which induces resistance to obesity. Biochim Biophys Acta. 2013;1828(2):455-60.
21. Hahm S, Mizuno TM, Wu TJ, et al. Targeted deletion of the Vgf gene indicates that the encoded secretory peptide precursor plays a novel role in the regulation of energy balance. Neuron. 1999;23(3):537-48.
22. Watson E, Fargali S, Okamoto H, et al. Analysis of knockout mice suggests a role for VGF in the control of fat storage and energy expenditure. BMC Physiol. 2009;9:19.
23. Bozdagi O, Rich E, Tronel S, et al. The neurotrophin-inducible gene Vgf regulates hippocampal function and behavior through a brain-derived neurotrophic factor-dependent mechanism. J Neurosci. 2008;28(39):9857-69.
24. Preeti H. Jethwa, Amy Warner, Kanishka N. Nilaweera, John M. Brameld, John W. Keyte, Wayne G. Carter, Neil Bolton, Michael Bruggraber, Peter J. Morgan, Perry Barrett, Francis J. P. Ebling, VGF-Derived Peptide, TLQP-21, Regulates Food Intake and Body Weight in Siberian Hamsters, Endocrinology, Volume 148, Issue 8, 1 August 2007, Pages 4044–4055, https://doi.org/10.1210/en.2007-0038
25. Bartolomucci A, La corte G, Possenti R, et al. TLQP-21, a VGF-derived peptide, increases energy expenditure and prevents the early phase of diet-induced obesity. Proc Natl Acad Sci USA. 2006;103(39):14584-9.
26. Mizoguchi T, Minakuchi H, Ishisaka M, Tsuruma K, Shimazawa M, Hara H. Behavioral abnormalities with disruption of brain structure in mice overexpressing VGF. Sci Rep. 2017;7(1):4691.
27. Hahm S, Fekete C, Mizuno TM, et al. VGF is required for obesity induced by diet, gold thioglucose treatment, and agouti and is differentially regulated in pro-opiomelanocortin- and neuropeptide Y-containing arcuate neurons in response to fasting. J Neurosci. 2002;22(16):6929-38.
28. Barrett P, Ross AW, Balik A, et al. Photoperiodic regulation of histamine H3 receptor and VGF messenger ribonucleic acid in the arcuate nucleus of the Siberian hamster. Endocrinology. 2005;146(4):1930-9.
29. Ross AW, Bell LM, Littlewood PA, Mercer JG, Barrett P, Morgan PJ. Temporal changes in gene expression in the arcuate nucleus precede seasonal responses in adiposity and reproduction. Endocrinology. 2005;146(4):1940-7.
30. Evans RM, Barish GD, Wang YX. PPARs and the complex journey to obesity. Nat Med. 2004;10(4):355-61.
31. Watson E, Hahm S, Mizuno TM, et al. VGF ablation blocks the development of hyperinsulinemia and hyperglycemia in several mouse models of obesity. Endocrinology. 2005;146(12):5151-63.

32. Bergen HT, Mizuno TM, Taylor J, Mobbs CV. Hyperphagia and weight gain after gold-thioglucose: relation to hypothalamic neuropeptide Y and proopiomelanocortin. Endocrinology. 1998;139(11):4483-8.
33. Bartolomucci A, Possenti R, Levi A, Pavone F, Moles A. The role of the vgf gene and VGF-derived peptides in nutrition and metabolism. Genes Nutr. 2007;2(2):169-80.
34. Choi SG, Wang Q, Jia J, et al. Characterization of Gonadotrope Secretoproteome Identifies Neurosecretory Protein VGF-derived Peptide Suppression of Follicle-stimulating Hormone Gene Expression. J Biol Chem. 2016;291(40):21322-21334.
35. Sadahiro M, Erickson C, Lin WJ, et al. Role of VGF-derived carboxy-terminal peptides in energy balance and reproduction: analysis of "humanized" knockin mice expressing full-length or truncated VGF. Endocrinology. 2015;156(5):1724-38.
36. Gonadotropin-releasing hormone (GnRH). (2009). British Journal of Pharmacology, 158(Suppl 1), S57–S58. https://doi.org/10.1111/j.1476-5381.2009.00501_32.x
37. Tsutsumi R, Webster NJ. GnRH pulsatility, the pituitary response and reproductive dysfunction. Endocr J. 2009;56(6):729-37.
38. Jiang H, Chen S, Lu N, et al. Reduced serum VGF levels were reversed by antidepressant treatment in depressed patients. World J Biol Psychiatry. 2017;18(8):586-591.
39. Cattaneo A, Sesta A, Calabrese F, Nielsen G, Riva MA, Gennarelli M. The expression of VGF is reduced in leukocytes of depressed patients and it is restored by effective antidepressant treatment. Neuropsychopharmacology. 2010;35(7):1423-8.
40. Thakker-varia S, Behnke J, Doobin D, et al. VGF (TLQP-62)-induced neurogenesis targets early phase neural progenitor cells in the adult hippocampus and requires glutamate and BDNF signaling. Stem Cell Res. 2014;12(3):762-77.
41. Jiang C, Lin WJ, Sadahiro M, et al. VGF function in depression and antidepressant efficacy. Mol Psychiatry. 2018;23(7):1632-1642.
42. Mizoguchi T, Hara H, Shimazawa M. VGF has Roles in the Pathogenesis of Major Depressive Disorder and Schizophrenia: Evidence from Transgenic Mouse Models. Cell Mol Neurobiol. 2019;39(6):721-727.
43. Casson RJ, Chidlow G, Ebneter A, Wood JP, Crowston J, Goldberg I. Translational neuroprotection research in glaucoma: a review of definitions and principles. Clin Experiment Ophthalmol. 2012;40(4):350-7.
44. Seidl SE, Potashkin JA. The promise of neuroprotective agents in Parkinson's disease. Front Neurol. 2011;2:68.
45. Dunnett SB, Björklund A. Prospects for new restorative and neuroprotective treatments in Parkinson's disease. Nature. 1999;399(6738 Suppl):A32-9.
46. Andersen JK. Oxidative stress in neurodegeneration: cause or consequence?. Nat Med. 2004;10 Suppl:S18-25.
47. Panahi Y, Mojtahedzadeh M, Najafi A, Rajaee SM, Torkaman M, Sahebkar A. Neuroprotective Agents in the Intensive Care Unit: -Neuroprotective Agents in ICU. J Pharmacopuncture. 2018;21(4):226-240.
48. Zhao Z, Lange DJ, Ho L, et al. Vgf is a novel biomarker associated with muscle weakness in amyotrophic lateral sclerosis (ALS), with a potential role in disease pathogenesis. Int J Med Sci. 2008;5(2):92-9.

49. Atkin JD, Farg MA, Walker AK, Mclean C, Tomas D, Horne MK. Endoplasmic reticulum stress and induction of the unfolded protein response in human sporadic amyotrophic lateral sclerosis. Neurobiol Dis. 2008;30(3):400-7.
50. Ilieva EV, Ayala V, Jové M, et al. Oxidative and endoplasmic reticulum stress interplay in sporadic amyotrophic lateral sclerosis. Brain. 2007;130(Pt 12):3111-23.
51. Shimazawa M, Tanaka H, Ito Y, et al. An inducer of VGF protects cells against ER stress-induced cell death and prolongs survival in the mutant SOD1 animal models of familial ALS. PLoS ONE. 2010;5(12):e15307.
52. Noda Y, Shimazawa M, Tanaka H, et al. VGF and striatal cell damage in in vitro and in vivo models of Huntington's disease. Pharmacol Res Perspect. 2015;3(3):e00140.
53. Shioda N, Han F, Fukunaga K. Role of Akt and ERK signaling in the neurogenesis following brain ischemia. Int Rev Neurobiol. 2009;85:375-87.
54. Disabato DJ, Quan N, Godbout JP. Neuroinflammation: the devil is in the details. J Neurochem. 2016;139 Suppl 2:136-153.
55. More SV, Kumar H, Kim IS, Song SY, Choi DK. Cellular and molecular mediators of neuroinflammation in the pathogenesis of Parkinson's disease. Mediators Inflamm. 2013;2013:952375.
56. Fehlings MG, Nguyen DH. Immunoglobulin G: a potential treatment to attenuate neuroinflammation following spinal cord injury. J Clin Immunol. 2010;30 Suppl 1:S109-12.
57. Domingues, Neuza & Estronca, Luís & Silva, João & Encarnação, Marisa & Mateus, Rita & Lobo-Silva, Diogo & Santarino, Inês & Saraiva, Margarida & Soares, Maria & Melo, Teresa & Jacinto, António & Vaz, Winchil & Vieira, Otilia. (2016). Cholesteryl hemiesters alter lysosome structure and function and induce proinflammatory cytokine production in macrophages. Biochimica et Biophysica Acta (BBA) - Molecular and Cell Biology of Lipids. 1862. 10.1016/j.bbalip.2016.10.009.
58. Alawieh A, Elvington A, Tomlinson S. Complement in the homeostatic and ischemic brain. Front Immunol. 2015;6:417.
59. 59.Stokowska A, Atkins AL, Morán J, Pekny T, Bulmer L, Pascoe MC, Barnum SR, Wetsel RA, Nilsson JA, Dragunow M, et al. Complement peptide C3a stimulates neural plasticity after experimental brain ischaemia. Brain. 2017; 140(2):353–69.
60. Strainic MG, Liu J, Huang D, et al. Locally produced complement fragments C5a and C3a provide both costimulatory and survival signals to naive CD4+ T cells. Immunity. 2008;28(3):425-35.
61. Mathern DR, Heeger PS. Molecules Great and Small: The Complement System. Clin J Am Soc Nephrol. 2015;10(9):1636-50.
62. Coulthard LG, Woodruff TM. Is the complement activation product C3a a proinflammatory molecule? Re-evaluating the evidence and the myth. J Immunol. 2015;194(8):3542-8.
63. Ma Y, Liu Y, Zhang Z, Yang GY. Significance of Complement System in Ischemic Stroke: A Comprehensive Review. Aging Dis. 2019;10(2):429-462.
64. Young KG, Yan K, Picketts DJ. C3aR signaling and gliosis in response to neurodevelopmental damage in the cerebellum. J Neuroinflammation. 2019;16(1):135.
65. Mariani MM, Kielian T. Microglia in infectious diseases of the central nervous system. J Neuroimmune Pharmacol. 2009;4(4):448-61.

66. El gaamouch F, Audrain M, Lin WJ, et al. VGF-derived peptide TLQP-21 modulates microglial function through C3aR1 signaling pathways and reduces neuropathology in 5xFAD mice. Mol Neurodegener. 2020;15(1):4.
67. Treede RD. The International Association for the Study of Pain definition of pain: as valid in 2018 as in 1979, but in need of regularly updated footnotes. Pain Rep. 2018;3(2):e643.
68. Colloca L, Ludman T, Bouhassira D, et al. Neuropathic pain. Nat Rev Dis Primers. 2017;3:17002.
69. Fairbanks CA, Peterson CD, Speltz RH, et al. The VGF-derived peptide TLQP-21 contributes to inflammatory and nerve injury-induced hypersensitivity. Pain. 2014;155(7):1229-37.
70. Soliman N, Okuse K, Rice ASC. VGF: a biomarker and potential target for the treatment of neuropathic pain?. Pain Rep. 2019;4(5):e786.
71. Chen YC, Pristerá A, Ayub M, et al. Identification of a receptor for neuropeptide VGF and its role in neuropathic pain. J Biol Chem. 2013;288(48):34638-46.
72. Strimbu K, Tavel JA. What are biomarkers?. Curr Opin HIV AIDS. 2010;5(6):463-6.
73. Soliman N, Hohmann AG, Haroutounian S, Wever K, Rice ASC, Finn DP. A protocol for the systematic review and meta-analysis of studies in which cannabinoids were tested for antinociceptive effects in animal models of pathological or injury-related persistent pain. Pain Rep. 2019;4(4):e766.
74. Llano DA, Devanarayan P, Devanarayan V. VGF in Cerebrospinal Fluid Combined With Conventional Biomarkers Enhances Prediction of Conversion From MCI to AD. Alzheimer Dis Assoc Disord. 2019;33(4):307-314.
75. Kumar A, Sidhu J, Goyal A, Tsao JW. Alzheimer Disease. In: StatPearls. Treasure Island (FL): StatPearls Publishing; 2020.
76. Sathe, G., Na, C.H., Renuse, S. et al. Phosphotyrosine profiling of human cerebrospinal fluid. Clin Proteom15, 29 (2018)
77. Lopez OL. Mild cognitive impairment. Continuum (Minneap Minn). 2013;19(2 Dementia):411-24.
78. Zarei S, Carr K, Reiley L, et al. A comprehensive review of amyotrophic lateral sclerosis. Surg Neurol Int. 2015;6:171.
79. Jaronen M, Goldsteins G, Koistinaho J. ER stress and unfolded protein response in amyotrophic lateral sclerosis-a controversial role of protein disulphide isomerase. Front Cell Neurosci. 2014;8:402.
80. Liu J, Wang F. Role of Neuroinflammation in Amyotrophic Lateral Sclerosis: Cellular Mechanisms and Therapeutic Implications. Front Immunol. 2017;8:1005.
81. Verma A. Altered RNA metabolism and amyotrophic lateral sclerosis. Ann Indian Acad Neurol. 2011;14(4):239-44.
82. Tao QQ, Wu ZY. Amyotrophic Lateral Sclerosis: Precise Diagnosis and Individualized Treatment. Chin Med J. 2017;130(19):2269-2272.
83. Pasinetti GM, Ungar LH, Lange DJ, et al. Identification of potential CSF biomarkers in ALS. Neurology. 2006;66(8):1218-22.
84. Bolton D, Gillett G. The Biopsychosocial Model of Health and Disease: New Philosophical and Scientific Developments [Internet]. Cham (CH): Palgrave Pivot; 2019.

85. James, S. L., Abate, D., Abate, K. H., Abay, S. M., Abbafati, C., Abbasi, N., Abbastabar, H., Abd-Allah, F., Abdela, J., Abdelalim, A., Abdollahpour, I., Abdulkader, R. S., Abebe, Z., Abera, S. F., Abil, O. Z., Abraha, H. N., Abu-Raddad, L. J., Abu-Rmeileh, N. M. E., Accrombessi, M. M. K., … Murray, C. J. L. (2018). Global, regional, and national incidence, prevalence, and years lived with disability for 354 diseases and injuries for 195 countries and territories, 1990–2017: a systematic analysis for the Global Burden of Disease Study 2017. The Lancet, 392(10159), 1789–1858.
86. Nibuya M, Morinobu S, Duman RS. Regulation of BDNF and trkB mRNA in rat brain by chronic electroconvulsive seizure and antidepressant drug treatments. J Neurosci. 1995;15(11):7539-47.
87. Yu H, Chen ZY. The role of BDNF in depression on the basis of its location in the neural circuitry. Acta Pharmacol Sin. 2011;32(1):3-11.
88. Egan MF, Kojima M, Callicott JH, et al. The BDNF val66met polymorphism affects activity-dependent secretion of BDNF and human memory and hippocampal function. Cell. 2003;112(2):257-69.
89. Duman RS, Monteggia LM. A neurotrophic model for stress-related mood disorders. Biol Psychiatry. 2006;59(12):1116-27.
90. Blumenthal JA, Smith PJ, Hoffman BM. Is Exercise a Viable Treatment for Depression?. ACSMs Health Fit J. 2012;16(4):14-21.
91. Shen H, Zhang L, Xu C, Zhu J, Chen M, Fang Y. Analysis of Misdiagnosis of Bipolar Disorder in An Outpatient Setting. Shanghai Arch Psychiatry. 2018;30(2):93-101.
92. Public Health Agency of Canada. Tracking Heart Disease & Stroke in Canada. 2009. Ottawa (Ontario): Public Health Agency of Canada; 2009 June 10
93. Lopez MF, Sarracino DA, Prakash A, et al. Discrimination of ischemic and hemorrhagic strokes using a multiplexed, mass spectrometry-based assay for serum apolipoproteins coupled to multi-marker ROC algorithm. Proteomics Clin Appl. 2012;6(3-4):190-200.
94. Khaku AS, Tadi P. Cerebrovascular Disease (Stroke). In: StatPearls. Treasure Island (FL): StatPearls Publishing; 2020.
95. Gravanis I, Tsirka SE. Tissue-type plasminogen activator as a therapeutic target in stroke. Expert Opin Ther Targets. 2008;12(2):159-70.
96. Jilani TN, Siddiqui AH. Tissue Plasminogen Activator. In: StatPearls. Treasure Island (FL): StatPearls Publishing; 2020.
97. Kannangara TS, Carter A, Xue Y, Dhaliwal JS, Béïque JC, Lagace DC. Excitable Adult-Generated GABAergic Neurons Acquire Functional Innervation in the Cortex after Stroke. Stem Cell Reports. 2018;11(6):1327-1336.
98. Pantoni L, Garcia JH, Gutierrez JA. Cerebral white matter is highly vulnerable to ischemia. Stroke. 1996;27(9):1641-6.
99. Dewar D, Underhill SM, Goldberg MP. Oligodendrocytes and ischemic brain injury. J Cereb Blood Flow Metab. 2003;23(3):263-74.
100. Gensert JM, Goldman JE. Endogenous progenitors remyelinate demyelinated axons in the adult CNS. Neuron. 1997;19(1):197-203.
101. Franklin RJ. Why does remyelination fail in multiple sclerosis?. Nat Rev Neurosci. 2002;3(9):705-14.
102. Li L, Harms KM, Ventura PB, Lagace DC, Eisch AJ, Cunningham LA. Focal cerebral ischemia induces a multilineage cytogenic response from adult subventricular zone that is predominantly gliogenic. Glia. 2010;58(13):1610-9.

103. Rafalski VA, Ho PP, Brett JO, et al. Expansion of oligodendrocyte progenitor cells following SIRT1 inactivation in the adult brain. Nat Cell Biol. 2013;15(6):614-24.
104. Zhang R, Chopp M, Zhang ZG. Oligodendrogenesis after cerebral ischemia. Front Cell Neurosci. 2013;7:201.
105. Li Y, Chen J, Zhang CL, et al. Gliosis and brain remodeling after treatment of stroke in rats with marrow stromal cells. Glia. 2005;49(3):407-17.
106. Zhang ZG, Chopp M. Neurorestorative therapies for stroke: underlying mechanisms and translation to the clinic. Lancet Neurol. 2009;8(5):491-500.
107. Zhang Y, Zhang H, Wang L, et al. Quetiapine enhances oligodendrocyte regeneration and myelin repair after cuprizone-induced demyelination. Schizophr Res. 2012;138(1):8-17.
108. Anrather J, Iadecola C. Inflammation and Stroke: An Overview. Neurotherapeutics. 2016;13(4):661-670.
109. Mo Y, Sun YY, Liu KY. Autophagy and inflammation in ischemic stroke. Neural Regen Res. 2020;15(8):1388-1396.
110. Yin J, Valin KL, Dixon ML, Leavenworth JW. The Role of Microglia and Macrophages in CNS Homeostasis, Autoimmunity, and Cancer. J Immunol Res. 2017;2017:5150678.
111. Wang P, Shao BZ, Deng Z, Chen S, Yue Z, Miao CY. Autophagy in ischemic stroke. Prog Neurobiol. 2018;163-164:98-117.
112. Sakamoto M, Miyazaki Y, Kitajo K, Yamaguchi A. VGF, Which Is Induced Transcriptionally in Stroke Brain, Enhances Neurite Extension and Confers Protection Against Ischemia In Vitro. Transl Stroke Res. 2015;6(4):301-8.
113. Bonni A, Ginty DD, Dudek H, Greenberg ME. Serine 133-phosphorylated CREB induces transcription via a cooperative mechanism that may confer specificity to neurotrophin signals. Mol Cell Neurosci. 1995;6(2):168-83.
114. Mantamadiotis T, Papalexis N, Dworkin S. CREB signalling in neural stem/progenitor cells: recent developments and the implications for brain tumour biology. Bioessays. 2012;34(4):293-300.
115. Watson BD, Dietrich WD, Busto R, Wachtel MS, Ginsberg MD. Induction of reproducible brain infarction by photochemically initiated thrombosis. Ann Neurol. 1985;17(5):497-504.
116. Schindelin J, Arganda-carreras I, Frise E, et al. Fiji: an open-source platform for biological-image analysis. Nat Methods. 2012;9(7):676-82.
117. Balkaya M, Kröber JM, Rex A, Endres M. Assessing post-stroke behavior in mouse models of focal ischemia. J Cereb Blood Flow Metab. 2013;33(3):330-8.
118. Baskin YK, Dietrich WD, Green EJ. Two effective behavioral tasks for evaluating sensorimotor dysfunction following traumatic brain injury in mice. J Neurosci Methods. 2003;129(1):87-93.
119. Farr TD, Liu L, Colwell KL, Whishaw IQ, Metz GA. Bilateral alteration in stepping pattern after unilateral motor cortex injury: a new test strategy for analysis of skilled limb movements in neurological mouse models. J Neurosci Methods. 2006;153(1):104-13.
120. Rao X, Huang X, Zhou Z, Lin X. An improvement of the 2ˆ(-delta delta CT) method for quantitative real-time polymerase chain reaction data analysis. Biostat Bioinforma Biomath. 2013;3(3):71-85.

121. Custo Greig, Luciano & Woodworth, Mollie & Galazo, María & Padmanabhan, Hari & Macklis, Jeffrey. (2013). Molecular logic of neocortical projection neuron specification, development and diversity. Nature reviews. Neuroscience. 14. 10.1038/nrn3586
122. Tatem KS, Quinn JL, Phadke A, Yu Q, Gordish-dressman H, Nagaraju K. Behavioral and locomotor measurements using an open field activity monitoring system for skeletal muscle diseases. J Vis Exp. 2014;(91):51785.
123. Barkho BZ, Zhao X. Adult neural stem cells: response to stroke injury and potential for therapeutic applications. Curr Stem Cell Res Ther. 2011;6(4):327-38.
124. Wang Y, Zhang H, He YW\. The Complement Receptors C3aR and C5aR Are a New Class of Immune Checkpoint Receptor in Cancer Immunotherapy. Front Immunol. 2019;10:1574.
125. Larpthaveesarp A, Ferriero DM, Gonzalez FF. Growth factors for the treatment of ischemic brain injury (growth factor treatment). Brain Sci. 2015;5(2):165-77.
126. Lindvall O, Kokaia Z. Neurogenesis following Stroke Affecting the Adult Brain. Cold Spring Harb Perspect Biol. 2015;7(11)
127. Gutiérrez-fernández M, Fuentes B, Rodríguez-frutos B, Ramos-cejudo J, Vallejo-cremades MT, Díez-tejedor E. Trophic factors and cell therapy to stimulate brain repair after ischaemic stroke. J Cell Mol Med. 2012;16(10):2280-90.
128. Yang L, Tucker D, Dong Y, et al. Photobiomodulation therapy promotes neurogenesis by improving post-stroke local microenvironment and stimulating neuroprogenitor cells. Exp Neurol. 2018;299(Pt A):86-96.
129. Lanfranconi S, Locatelli F, Corti S, et al. Growth factors in ischemic stroke. J Cell Mol Med. 2011;15(8):1645-87.
130. Zhang RL, Zhang ZG, Zhang L, Chopp M. Proliferation and differentiation of progenitor cells in the cortex and the subventricular zone in the adult rat after focal cerebral ischemia. Neuroscience. 2001;105(1):33-41.
131. Lu C, Wu X, Ma H, et al. Optogenetic Stimulation Enhanced Neuronal Plasticities in Motor Recovery after Ischemic Stroke. Neural Plast. 2019;2019:5271573.
132. Ma Y, Wang K, Pan J, et al. Induced neural progenitor cells abundantly secrete extracellular vesicles and promote the proliferation of neural progenitors via extracellular signal-regulated kinase pathways. Neurobiol Dis. 2019;124:322-334.
133. Tang C, Wang M, Wang P, Wang L, Wu Q, Guo W. Neural Stem Cells Behave as a Functional Niche for the Maturation of Newborn Neurons through the Secretion of PTN. Neuron. 2019;101(1):32-44.e6.
134. Zhao SC, Ma LS, Chu ZH, Xu H, Wu WQ, Liu F. Regulation of microglial activation in stroke. Acta Pharmacol Sin. 2017;38(4):445-458.
135. Raggi F, Pelassa S, Pierobon D, et al. Regulation of Human Macrophage M1-M2 Polarization Balance by Hypoxia and the Triggering Receptor Expressed on Myeloid Cells-1. Front Immunol. 2017;8:1097.
136. Mocco J, Wilson DA, Komotar RJ, et al. Alterations in plasma complement levels after human ischemic stroke. Neurosurgery. 2006;59(1):28-33.
137. Rock RB, Gekker G, Hu S, et al. Role of microglia in central nervous system infections. Clin Microbiol Rev. 2004;17(4):942-64, table of contents.
138. Rahpeymai Y, Hietala MA, Wilhelmsson U, et al. Complement: a novel factor in basal and ischemia-induced neurogenesis. EMBO J. 2006;25(6):1364-74.

139. Huang C, Jacobson K, Schaller MD. MAP kinases and cell migration. J Cell Sci. 2004;117(Pt 20):4619-28.
140. Tanimura S, Takeda K. ERK signalling as a regulator of cell motility. J Biochem. 2017;162(3):145-154.
141. Sun J, Nan G. The extracellular signal-regulated kinase 1/2 pathway in neurological diseases: A potential therapeutic target (Review). Int J Mol Med. 2017;39(6):1338-1346.

Appendix

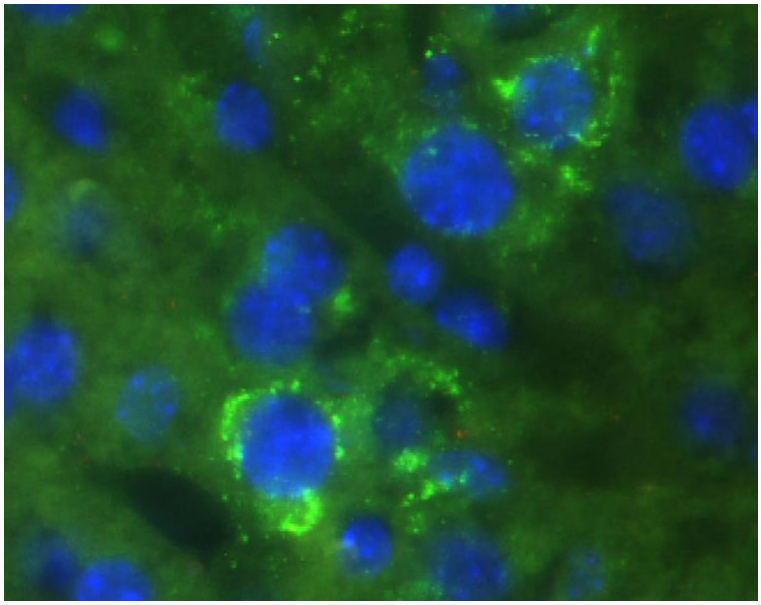

Appendix A. Adenoviral-VGF expression in adult WT mice post-intravenous delivery. Immunohistological staining of liver tissue sections in C57BL/6J WT mice two days post-injection. VGF antibody was used to detect VGF expression (green) co-labelled with DAPI. FOV = 100X.

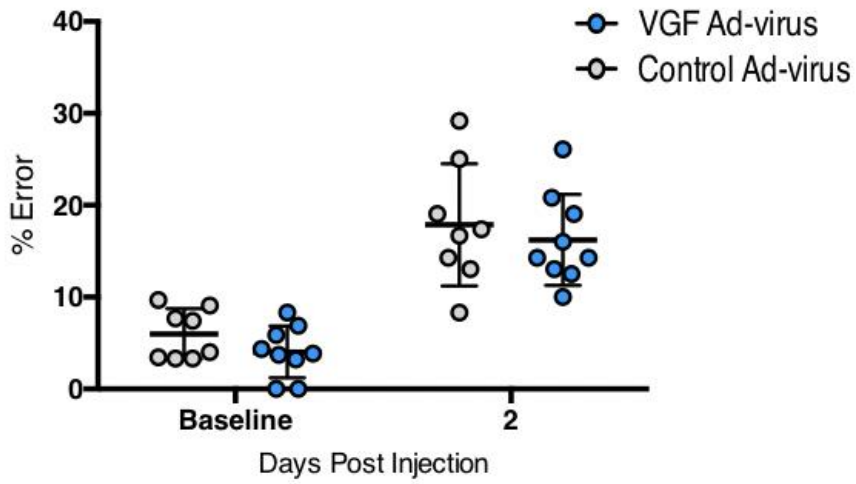

Appendix B. Behavioural analysis of adenoviral injected mice 2 days post-injection. Quantification of % Error in Horizontal Ladder behavioral test pre- and post-photothrombosis and injection of VGF-adenovirus on 8-week-old WT mice. (n= 8 WT+ControlAd, 9 WT+VGFAd).

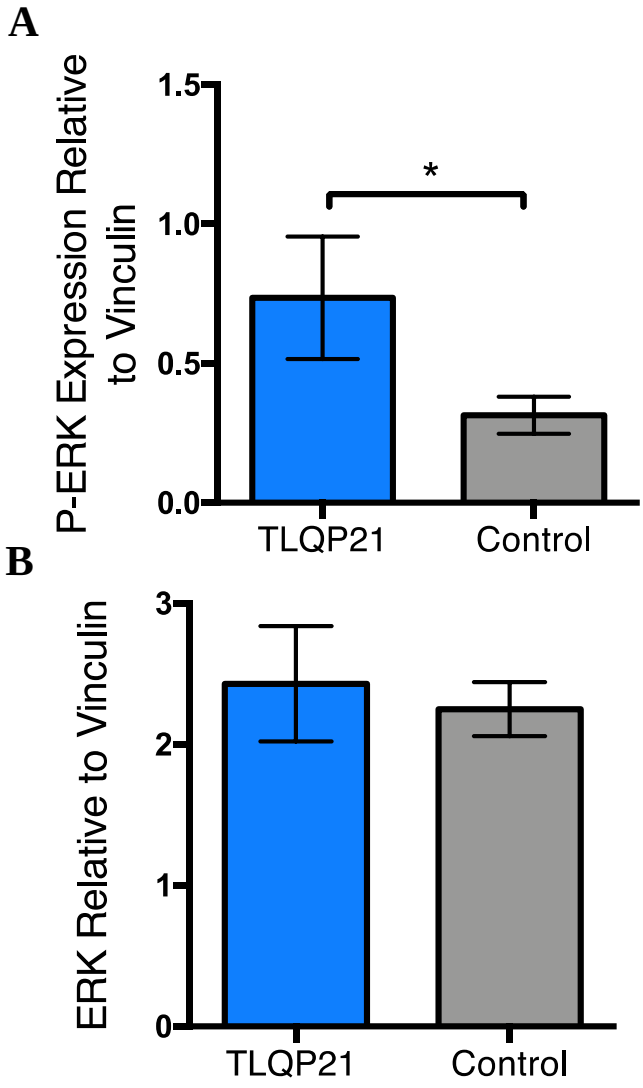

Appendix C. Western blot analysis of resident ERK and P-ERK in TLQP-21 treated Raw264.7 cells. A. Quantification of **Figure 20A**, P-ERK compared to vinculin control. P-value = 0.0104 (n=3 TLQP21, 3 Control) B. Quantification of **Figure 20A**, ERK compared to vinculin control. No significant difference. (n=3 TLQP21, 3 Control)

Curriculum Vitae

Hannah Gillis

EDUCATION/TRAINING/SKILLS

University of Ottawa, Ottawa, Ontario 2017-2020
The Ottawa Hospital Research Institute, Regenerative Medicine Department
Graduate Student

Roger Neilson House, Ottawa, Ontario 2017-Present
Pediatric Palliative Care Volunteer & Youth Counsellor

Mothercraft Ottawa, Ottawa, Ontario 2017-Present
Birth Companion (trained doula for vulnerable populations)

University of Ottawa, Ottawa, Canada 2013-2017
BSc. Honours Biomedical Science

TCPS 2: CORE (Course on Ethics Training) - Certification 2015
Children's Hospital of Eastern Ontario

WORK EXPERIENCE

Privacy Analytics 2019-Present
Clinical Trials Data Analyst – Clinical Trials Transparency Team

Canadian Foundation for Healthcare Improvement 2019
External Consultant – Home and Community Care Literature Review

The Ottawa Hospital Research Institute 2017
Research Assistant

University of Ottawa, Ottawa, Canada 2015-2019
Student Ambassador
Exam Proctor

Learning Enrichment Foundation 2016
Summer Policy Intern

Second People's Teaching Hospital of Changzhou, Changzhou, China 2015
Health System Analyst Intern, Cansbridge Fellowship

Canadian Foundation For Healthcare Improvement, Ottawa, Canada 2014
Collaborations For innovation and Improvement Intern

VOLUNTEER COMMITTEES

Canadian Partnership for Stroke Recovery 2017-Present
Trainee (MSc.)

Lets Talk Science, Ottawa, Ontario 2017-Present
Volunteer

LORAN Scholars Association 2013-Present
Alumni

Children's Hospital of Eastern Ontario, Ottawa, Ontario 2014-2017
Research Institute S.U.P.P.O.R.T. member

Around the Campfire Volunteer
2016- 2017
Music and Rhythm therapy for children with disabilities
St. Joe's Supper table Volunteer and Committee member, Ottawa 2013-2017
Social Media Coordinator
Making Waves, Ottawa, Canada 2013 – 2015
Volunteer Swimming Instructor for Children with Special Needs

AWARDS & ACCOMPLISHMENTS

- **BMI Seminar Day, MSc. Prize, uOttawa 2019**
- **2nd Place Poster (MSc.) BMI Research Day, uOttawa 2018**
- **Cansbridge Fellowship Recipient 2015**
- **National Loran Scholarship Recipient 2013**
- **University of Ottawa Entrance Scholarship 2013**
- **Governor General of Canada Medal for Academic Excellence 2013**
- **Highest Overall Academic Average, Honours with Distinction 2013**
- **Provincial Minister of Justice Award for Leadership in Crime Prevention 2013**
- **Lieutenant Governor's medal 2012**
- **Featured in 'The Canadian Press', (Teen Relationships/Social Networking) 2012**

SCIENTIFIC CONTRIBUTIONS

- **Participant/Presenter**
    - 18th International Fragile X & Related Neurodevelopmental Disorders Workshop, Saint-Alexis-des-Monts, QC (2017)
    - Stem Cell Symposium, Ottawa Hospital Research Institute (2017,2018)
    - Stroke Program in Neurorecovery workshop (Calgary, 2017; Ottawa, 2018)
    - Biochemistry, Microbiology and Immunology Research Day (Ottawa, 2017,2018, 2019)
    - Ottawa Hospital Research Institute Day 2019, Speaker (Ottawa – 2019)
    - Brain Health Research Day (Ottawa 2016, 2017, 2018, 2019)